SULFUR-ISOTOPE VARIATIONS IN SULFIDE MINERALS FROM MASSIVE SULFIDE DEPOSITS OF THE NORTHERN APENNINE OPHIOLITES: INORGANIC AND BIOGENIC CONSTRAINTS

Giorgio Garuti[*,✉], **Pura Alfonso**[**], **Joaquín A. Proenza**[***] and **Federica Zaccarini**[*]

[*]   *Department Angewandte Geowissenschaften und Geophysik, Montanuniversität Leoben, Austria.*
[**]   *Departament d'Enginyeria Minera i Recursos Naturales, Universitat Politecnica de Catalunya. UPC, Barcelona, Spain.*
[***] *Departament de Crystallografia, Mineralogia i Depòsits Minerals, Universitat de Barcelona, España.*
[✉]   *Corresponding author, e-mail: giorgiogaruti@unileoben.ac.at*

ABSTRACT

Sulfur isotope analysis of sulfide minerals has been carried out for the first time on ore samples from Volcanic-associated Massive Sulfide (VMS) deposits in Tethyan Jurassic ophiolites of the Northern Apennine. The average $\delta^{34}S$ value is +5.2‰ in pyrite (n. 22), +6.7‰ in chalcopyrite (n. 23), +6.1‰ in sphalerite (n. 9), and 4.6‰ in pyrrhotite (n. 2). The overall average $\delta^{34}S$ of +5.9‰ (n = 30, σ = 3.7) is consistent with data from other sulfide deposits of the Eastern Mediterranean Tethys, although the Apennine ores display a distinctive range from +11.4‰ to the negative field (min. -2.9). The highest $\delta^{34}S$‰ values are found in stockwork veins crosscutting basalt and gabbro, and in stratabound ores within basalt (av., +8.9‰). The $\delta^{34}S$ decreases in serpentinite-hosted stockwork veins (av., +5.8‰) and in stratiform deposits lying on ancient seafloors (av., +2.5‰), in which the negative values were detected. Inorganic reduction of seawater sulfate is assumed to be the primary source of sulfur in the deposits, with some exception however. The low $\delta^{34}S$ values of serpentinite-hosted veins indicate mixing with sulfur derived from the leaching of magmatic sulfides (av., $\delta^{34}S$ = +0.8‰). The negative values detected in seafloor-stratiform ores correlate with sulfide textures indicative of the activity of sulfate-reducing bacteria causing preferential fractionation of the light sulfur isotope. The sulfur isotope variations observed in the Northern Apennine VMS deposits reflect the influence of the different environments of sulfide deposition (seafloor vs. sub-seafloor) and different lithologies of the host rocks (basalt vs. serpentinite).

INTRODUCTION

Sulfide deposits located in the Northern Apennine of Italy have been known as a workable source of copper since 3500 BC, thus providing evidence for the earliest copper exploitation in Western Europe (Maggi and Pearce, 2005). Between the Middle Age and the 18th century, copper was extracted cyclically, becoming a major commodity only in the Industrial Era. From 1850 to 1910, several new deposits were discovered and intensively mined in eastern Liguria, yielding more than 1.5 Mt of ore with an average grade of 2-7% Cu. After a short period of decline, mining activities started again during "Autarky" (1936) and lasted until the early seventies, when the mines at Libiola (eastern Liguria), Vigonzano and Ferriere (Emilia Romagna) were definitively closed (Moretti, 1937; Violi Guidetti, 1968; Galli and Penco, 1996; Pipino, 2003).

The most important copper deposits are associated with the Western Alps and Northern Apennine ophiolites (Fig. 1), which represent fragments of the sub-oceanic lithosphere that floored the Liguria-Piedmont Tethys. This embryonic ocean formed by divergence of the European and the Adriatic Plates in Jurassic times, and closed between Late Cretaceous and Early Eocene (see references in Piccardo et al., 2002). Continental rifting in a slow-spreading regime initially caused intrusion of MORB-type gabbroic bodies into the upper mantle (Tribuzio et al., 2000; 2004), and subsequently evolved into ocean opening (Piccardo et al., 2002). Tectonic denudation allowed the peridotite-gabbro basement to be exposed and eroded on the ocean floor, before the outflow of MORB-type pillow lava and the deposition of pelagic sediments (Abbate et al., 1970; Cortesogno et al., 1975; Bortolotti and Gianelli, 1976; Barrett, 1982; Lemoine et al.,

1987; Lagabrielle and Lemoine, 1997). Upper Jurassic radiolarian cherts with Mn deposits cover the volcanic rocks (Bonatti et al., 1976; Marcucci and Passerini, 1991; Cabella et al., 1998). Recession of the seafloor from the axial rifting zone and the decrease of magma extrusion led to progressive burial of the igneous-volcanic basement and cherts under carbonatic-siliciclastic sediments (Palombini Shales and Calpionella Limestones) in the Cretaceous, passing upward to various types of arenaceous turbidites (Late Cretaceous to Paleocene).

Ophiolites of the Northern Apennine differ from coeval ophiolites of the Western Alps because of the common lack of eclogite- and blueschist-facies orogenic metamorphism (Dal Piaz, 1974a; 1974b; Sandrone et al., 1986). They generally display the effects of low-grade oceanic metamorphism and syn-orogenic deformation caused by north-eastwards thrusting onto the Adria continental margin (Cortesogno et al., 1975). Basalts are spilitized to variable extents (Capedri and Toscani, 2000 and references therein). The highest degree of alteration is observed in the surroundings of stockwork-vein bodies (see below) where the basalt is totally transformed into a felt aggregate of spiky albite crystals, with interstitial chlorite, epidote and Fe-Ti oxides (Zaccarini and Garuti, 2008). Hydrothermal alteration of gabbros produced a low temperature secondary assemblage consisting of sericitized-saussuritized plagioclase, albite, tremolite, chlorite and calcite (i.e., Montecreto ophiolite). Basalts, gabbros and serpentinized peridotites of mantle origin from eastern Liguria (away from areas with sulfide ore deposits) are enriched in ^{18}O, indicating isotopic exchange with normal seawater below 200°C, at or near the seafloor (Barrett and Friedrichson, 1989). Palombini Shales from the sedimentary cover in the same area (Colli-Tavarone and Bracco-
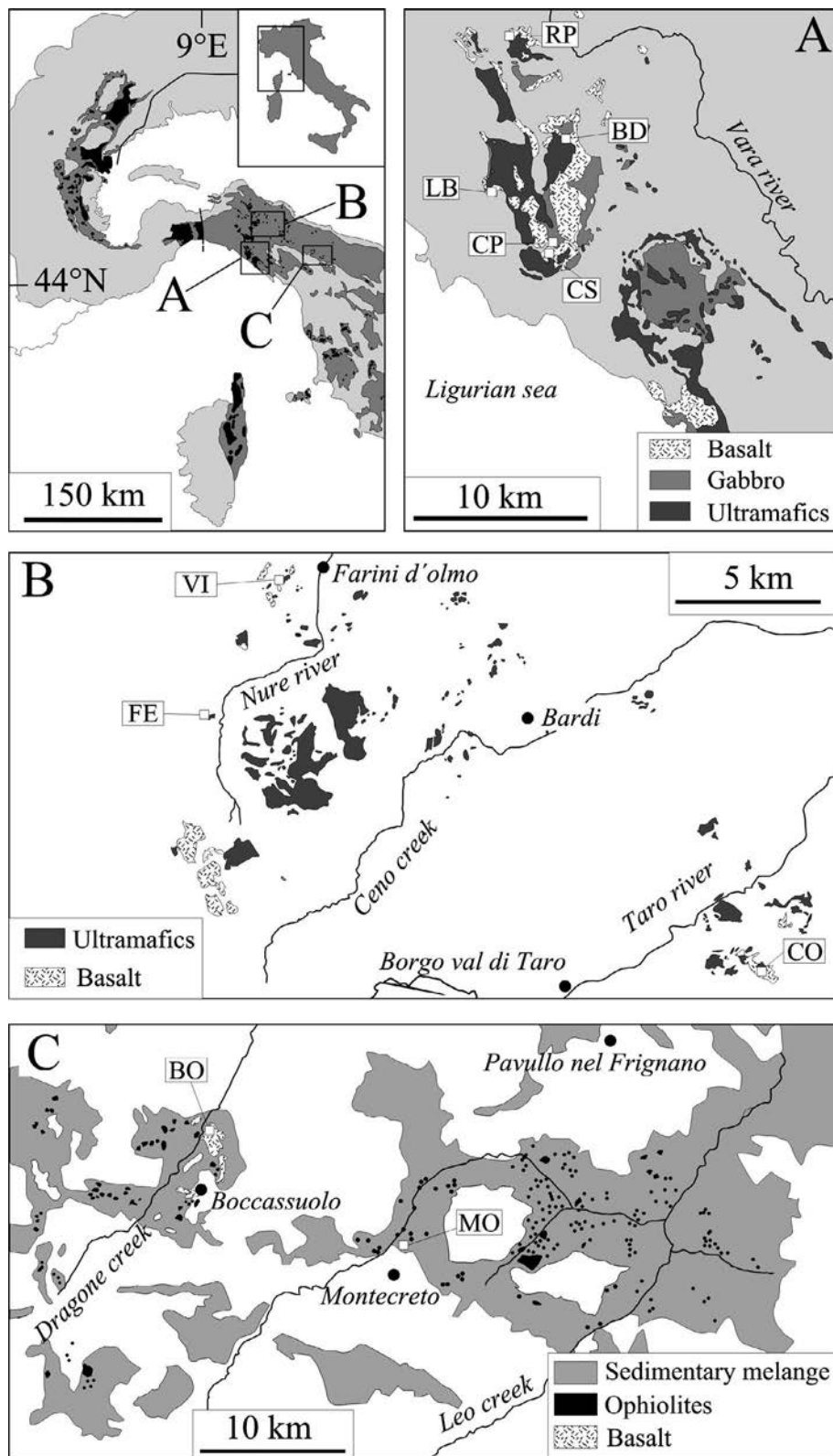
44

Fig. 1 - Location of the investigated VMS deposits in the Northern Apennine. Left top square: simplified map of Piedmont-Ligurian Units (dark grey) and ophiolite complexes (black) in the Northern Apennine and Western Alps. A) Eastern Liguria, RP- Reppia, BD- Monte Bardeneto, LB- Libiola, CP- Campegli, CS- Casali-Monte Loreto; B) Western Emilia Romagna, CO- Corchia, VI- Vigonzano, FE- Ferriere; C) Central Emilia Romagna, BO- Boccassuolo, MO- Montecreto. Modified after Zaccarini and Garuti (2008) and Bertolani and Capedri (1966).

Val Graveglia Units) experienced maximum temperatures and pressures of 160-250°C and 2-3 kb, respectively, compatible with conditions of extreme burial diagenesis during orogenic evolution (Leoni et al., 1998).

The sulfide deposits of the Northern Apennine are characterized by the metal assemblage Fe-Cu-Zn typical of ophiolite-hosted Volcanic Massive Sulfide (VMS) deposits (Galley and Koski, 1999). They consist of the hydrothermal ore assemblage pyrite-chalcopyrite-sphalerite with or without pyrrhotite, galena, magnetite and other accessory ore minerals (linneite, millerite, marcasite, covellite, gold, silver, acanthite, freibergite, ilmenite, rutile, uraninite, hydroromarchite). Quartz, calcite and chlorite are major gangue minerals, along with accessory siderite, epidote, titanite, apatite and zircon (Bertolani, 1952; 1953; 1959; 1962; Ferrario, 1977; Ferrario and Garuti, 1980; Garuti and Zaccari-

ni, 2005; Zaccarini, 2006; Zaccarini and Garuti, 2008).

Stratigraphic relationships (Fig. 2) suggest that formation of the sulfide deposits occurred in different stages during evolution of the Ligurian basin (Garuti et al., 2008a). Initially, sulfur-rich hydrothermal fluids venting onto the ocean-floor deposited conformable-stratiform ore bodies on the serpentinite breccia derived from sea-floor erosion of the mantle basement (Type 1). The mineralized stockwork-veins of Types 4a and 4b provide evidence that convective hydrothermal cells were emplaced within the mantle substrate, after its exposure at the ocean floor. The stratiform deposits of Type 1 are invariably covered by pillow basalt flows, suggesting that hydrothermal circulation was probably triggered by heat emanating from the upraising basaltic magma (Garuti et al., 2008a). Hydrothermal activity continued during and after basalt extrusion, leading to precipitation of sulfides on the volcanic ocean-floor (Type 2), as well as to deposition of stratabound ore bodies (Type 3) and stockwork veins (Type 4c) within the volcanic rocks.

The Northern Apennine deposits represent a rare example of seafloor-stratiform, stratabound, and sub-seafloor stockwork ore-bodies associated with both the ultramafic basement and the basalt volcanic cover in one single ophiolite sequence. Because of the lack of a significant metamorphic overprint, they yielded a unique opportunity to investigate how and to what extent the different depositional settings (seafloor vs. sub-seafloor) and host rocks (basalt vs. serpentinite) have influenced the primary mineralogy and composition of the sulfide ore (Garuti and Zaccarini, 2005; Zaccarini, 2006; Zaccarini and Garuti, 2008). Preliminary observations suggest that depositional setting and host rock composition may have influenced also the sulfur isotopic composition of the ore (Garuti et al., 2007). In this paper we report the results of the first systematic study of sulfur isotopes in sulfide minerals from selected VMS deposits of the Northern Apennine, considered as representatives of the various depositional settings described.

ANALYTICAL PROCEDURES

Sulfur isotopes analyses were performed on single sulfide minerals: pyrite (32 grains from 26 samples), chalcopyrite (28 grains from 24 samples), sphalerite (9 grains from 9 samples) and pyrrhotite (2 grains from 2 samples). The sulfide minerals were separated by scratching the surface of polished sections with a sharp needle, and picked up from the polished section under the microscope. The obtained grains had a minimum size of several tens of microns therefore the possible influence of micro-impurities could not be avoided. This circumstance caused negligible contamination in the isotopic analysis of pyrite and chalcopyrite which usually contain minor micro-inclusions, but was a serious limitation in the case of sphalerite. The mineral is invariably clouded with minute inclusions of chalcopyrite, down to less than $1\mu m$ in size, known as the "chalcopyrite-disease" texture. Sphalerite is so densely spotted with chalcopyrite inclusions as to affect even the results of electron microprobe analysis (see the Sulfide Mineral Chemistry section).

Two isotopic determinations were repeated for pyrite and chalcopyrite in selected samples. The isotopic analyses were carried out at the Serveis Científic-Tècnics (University of Barcelona, Spain), using a combustion apparatus equipped with Delta C Finnigan MAT, continuous flow, isotope-ratio mass spectrometer, and TC-EA elemental analyzer, following the method of Giesemann et al. (1994). The results are given as $\delta^{34}S‰$ values relative to the Cañon del Diablo Troilite (CDT) standard. The analytical precision (2σ) is within ±0.2‰.

In order to characterize the compositions of the investigated sulfide ores, bulk-rock concentrations of Cu, Zn, Ni, Co, Cr, Au, Ag and U, performed at the Actlabs Laboratory, Thornhill, Ontario, were made available by Garuti and Zaccarini (2005) and Zaccarini and Garuti (2008). Textural relationships, mineral assemblages and composition of the sulfide minerals were studied by optical and electronic microscopy, and electron microprobe analysis, at the Eugen
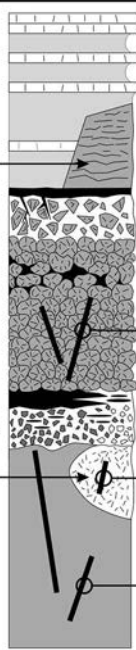

Lithology		Ore type	Examples
Palombini shale			
Chert			
Seafloor pillow breccia		Type-2 stratiform sulfide	Reppia II Corchia
Pillow basalt		Type-3 stratabound sulfide	Libiola
		Type-4c stockwork veins	Boccassuolo Montecreto Casali-Monte Loreto Reppia I Monte Bardeneto
Seafloor serpentinite breccia		Type-1 stratiform sulfide	
Intrusive gabbro		Type-4b stockwork veins	Campegli
Serpentinite		Type-4a stockwork veins	Ferriere Vigonzano

Fig. 2 - Idealized schematic stratigraphy of VMS deposits of the Northern Apennine (not to scale). Structural relations indicate that the serpentinite-gabbro basement was exposed and eroded at the seafloor prior to outflow of pillow basalts. The Reppia II deposit is covered with chert, the Corchia deposit with Palombini Shales. See Garuti et al. (2008a) for geological details.

Stumpfl Microprobe Laboratory (University of Leoben). Electron microprobe analyses were obtained with a Jeol Superprobe JXA-8200, operated at 15 kV accelerating voltage, 10 nA beam current, ~1 μm beam diameter, and counting times of 20 and 5 seconds for peak and backgrounds, respectively. Raman spectroscopy was used to quickly check the mineralogical nature of Fe-oxides.

SAMPLES DESCRIPTION

A total of 34 samples of sulfide ore coming from 11 mining sites in eastern Liguria and western to central Emilia Romagna were selected for the isotopic analysis (Fig. 1A, B, C). All the samples were collected away from supergene weathered zones. Care was taken to investigate representatives of all the ore types, covering the most outstanding textural variations displayed by single ore deposits. In order to test the possible influence of "sulfide leaching" from the ultramafic basement, the isotopic composition of magmatic sulfides from one small Fe-Cu-(Ni) deposit associated to serpentinite was investigated. Sulfides disseminated in the serpentinite could not be used for this purpose due to the extremely low sulfur content of the ultramafic rocks (< 200 ppm), and the high degree of alteration of sulfide grains. Provenance and mineralogy of the analyzed samples are summarized in Tables 1 and 2, together with bulk-rock compositional data. Table 3 reports the results of electron microprobe analysis on selected sulfide minerals.

Local geologic setting of the investigated deposits

The stratiform deposits consist of concordant, tabular bodies up to 2-4 meters in thickness, having massive structure at the contact with the hanging-wall rocks, and grading into disseminated ore downwards.

Type 1: The stratiform deposits of Monte Bardeneto and Reppia I (eastern Liguria, Fig. 1A) are associated with the seafloor serpentinite breccia that marks the transition between serpentinite basement and pillow basalt (Fig. 3A).

The host breccia consists of serpentinite clasts along with minor fragments of sandstone and micritic limestone (basaltic clasts are absent), embedded in a sandy matrix of quartz, calcite, chlorite and minute rock fragments, characterized by graded bedding and other sedimentary textures (Ferrario and Garuti, 1980; Garuti and Zaccarini, 2005; Garuti et al., 2008a). Five samples of massive ore were collected: three from Monte Bardeneto (BD6, BD8, BDX) and two from Reppia I (RP1, RP2B).

Type 2: The stratiform deposits of Reppia II (eastern Liguria, Fig. 1A) and Corchia (western Emilia Romagna, Fig. 1B) occur in basalt breccia at the top of the pillow basalt unit. They are stratigraphically overlain by pelagic sediments consisting of Palombini Shales in olistostrome facies at Corchia (Fig. 3B), and by chert and Calpionella Limestones at Reppia II (Fig. 3C). The host breccia is composed of fragmented pillows surrounded by a fine-grained matrix of quartz, carbonate, chlorite and fragments of chert and clay minerals (Garuti and Zaccarini, 2005; Garuti et al., 2008a). Six samples of massive sulfide ore were examined: two from Reppia II (RP12, RP14) and four from Corchia (CO1, CO8, CO12, CO17).

Type 3: The stratabound sulfide deposit of Libiola (eastern Liguria, Fig. 1A) consists of a suite of massive sulfide lenses stacked one on the other, hosted in a huge dome of pillow basalt, underlain and partly overthrust by massive serpentinite and laminated gabbro (Bertolani, 1952; Ferrario and Garuti, 1980). At the footwall, massive ore bodies grade to a network of sulfide infiltrating among and into fragmented pillows (Fig. 3D), giving rise to an interstitial ore that grades into a reticulate of millimetric veins, filling cracks and fissures within completely chloritized basalt (stringer ore). Two samples representing the massive (LB13) and stringer ore (LB12), respectively, were selected for isotopic analysis.

Type 4a: Two examples of stockwork-veins hosted in serpentinite were studied in the old mines of Ferriere and Vigonzano (western Emilia Romagna, Fig 1B). The deposit of Ferriere consists of a network of quartz-carbonate-chlorite-siderite veins vertically emplaced into a huge serpentinite block, tectonically embedded in a sedimentary mélange

Table 1 - Provenance and location of the investigated samples from VMS deposits of the Northern Appennines ophiolites.

Deposit Type/Provenance	Sample labels	Location	GPS coordinates	
Hydrothermal Volcanic Massive Sulfides emplaced during Jurassic ocean opening				
Type 1) Stratiform ore in seafloor serpentinite breccia covered by pillow basalt				
Monte Bardeneto (eastern Liguria)	BD6, BD8, BDX	Upper mining works, alt. 778m	N 44°20' 376	E 09°29' 400
Reppia I (eastern Liguria)	RP1, RP2B	Main dump, alt. 625 m	N 44°22' 905	E 09°27' 451
Type 2) Stratiform ore in seafloor basalt breccia covered by pelagic sediments				
Reppia II (eastern Liguria)	RP12, RP14	Trench on the road, alt. 845 m	N 44°23' 228	E 09°27' 392
Corchia (western Emilia Romagna)	CO1	"Cantiere Donnini", alt. 770m	N 44°29' 780	E 09°55' 276
	CO8, CO12, CO17	"Cantiere Speranza"	N 44°29' 776	E 09°55' 272
Type 3) Stratabound deposits in pillow basalt				
Libiola (eastern Liguria)	LB12, LB13	Open pit	N 44°18' 240	E 09°26' 938
Type 4a) Stockwork veins in serpentinite				
Ferriere (western Emilia Romagna)	FE2	"Grondone" (gallery N° 4)	N 44°39' 481	E 09°28' 952
	FE13	"Grondone" (outcrop) alt. 860m	N 44°39' 410	E 09°28' 916
Vigonzano (western Emilia Romagna)	VI13	"Rocca Lagona"	N 44°42' 100	E 09°31' 828
	VI18, VI24	"Cantiere Vaie", alt. 785m		
Type 4b) Stockwork veins in gabbro				
Campegli (eastern Liguria)	CP1, CP3	Prospect, alt. 250 m	N 44°16' 909	E 09°29' 330
Type 4c) Stockwork veins in basalt				
Montecreto (central Emilia Romagna)	MO11	"Cà Marsiglio" gallery, alt. 620m	N 44°15' 969	E 10°43' 744
Boccassuolo (central Emilia Romagna)	BO6	"Labirintica" gallery, alt. 704	N 44°18' 345	E 10°37' 173
	BO33	"La Pioppaccia" (dump), alt.685m		
	BO53	"Miniera dei due livelli"	N 44°17' 977	E 10°37' 171
	BO91, BO93	"Cinghi" quarry, alt. 874m		
	BO96, BO97, BO98	"Filone Omar", alt. 880m	N 44°17' 924	E 10°37' 370
Casali-Monte Loreto (eastern Liguria)	CS5	Adit, alt. 355 m	N 44°16' 229	E 09°29' 690
Magmatic sulfide deposits emplaced in the ultramafic basement of the Ligurides before the Jurassic ocean-opening				
Stratiform ore concordantly emplaced in massive serpentinite				
Corchia (western Emilia Romagna)	COPO1, COPO2, COPO3, COPO4	"Il Pozzo" shaft, alt. 1065m	N 44°29' 927	E 09°54' 493

Table 2 - Mineralogy and bulk-rock metal concentration samples from VMS deposits of the Northern Appennines ophiolites.

Deposit Type / Locality / Sample	Ore type 1	Ore assemblage 2	Gangue minerals	% Cu	% Zn	ppm Ni	ppm Co	ppm Cr	ppb Au	ppm Ag	ppm U
Hydrothermal Volcanic Massive Sulfides emplaced during Jurassic ocean opening											
Type 1) Stratiform ore in seafloor serpentinite breccia covered by pillow basalt											
Monte Bardeneto (eastern Liguria)											
BD6	massive	Py-Po-Cp-(Sph-Mgt-Chr)	Cal-Qz-Chl-Sid-Serp	3.12	0.01	277	655	420	259	0.4	2.8
BD8	massive	Py-Po-Cp-Mgt-(Chr)	Cal-Qz-Chl-Serp	1.40	0.02	524	183	403	149	0.3	2.2
BDX	massive	Py-Po-Cp-(Sph)	Qz-Cal-Chl-Serp	1.72	0.76	432	343	161	461	6.7	4.7
Reppia I (eastern Liguria)											
RP1	massive	Py-Po-Cp-(Chr-Mgt)	Qz-Cal-Sid-Chl-Serp	1.80	0.04	879	4030	881	80	0.4	0.0
RP2B	massive	Py-Po-Cp-(Chr-Mgt)	Qz-Cal-Sid-Chl-Serp	1.67	0.02	259	334	212	27	0.3	1.1
Type 2) Stratiform ore in seafloor basalt breccia covered by pelagic sediments											
Corchia (western Emilia Romagna)											
CO1	massive	Py-Cp-(Sph)	Qz-Cal-Sid-Chl	5.81	0.27	932	2860	28	3070	6.0	2.5
CO12	massive	Py-Cp-(Sph)	Qz-Cal-Sid-Chl	0.98	0.14	287	1230	13	173	13	3.5
CO8	massive	Sph-(Py-Cp-Po)	Qz-Cal-Sid-Chl	0.58	32	33	1700	5	63	130	0.0
CO17	massive	Sph-(Py-Cp-Po)	Qz-Cal-Sid-Chl	n.a.	n.a.	n.a.	n.a.	n.a.	n.a.	n.a.	n.a.
Reppia II (eastern Liguria)											
RP12	massive	Py-Cp-(Sph)	Qz-Cal-Sid-Chl	0.07	0.01	36	110	9	342	0.7	0.0
RP14	massive	Py-Cp-(Sph)	Qz-Cal-Chl	0.90	0.01	172	178	14	475	1.0	0.0
Type 3) Stratabound deposits in pillow basalt											
Libiola (eastern Liguria)											
LB12	stringers	Py-Cp-(Sph-Po)	Qz-Cal-Chl	0.87	0.02	66	63	143	18	1.1	4.2
LB13	massive	Cp-(Sph-Py)	Qz	26.4	0.24	39	137	31	220	1.9	0.5
Type 4a) Stockwork veins in serpentinite											
Ferriere (western Emilia Romagna)											
FE2	semi-massive	Py-Cp-(Chr-Mgt)	Qz-Chl-Serp	n.a.	n.a.	n.a.	n.a.	n.a.	n.a.	n.a.	n.a.
FE13	massive	Py-Po-Cp-Mgt	Qz-Cal-Sid	8.69	0.06	511	401	232	80	5.3	2.1
Vigonzano (western Emilia Romagna)											
VI13	massive	Py-(Cp-Po-Sph)	Qz-Chl	0.24	0.01	622	168	32	32	1.1	0.0
VI18	semi-massive	Py-(Cp-Po-Sph-Mgt-Hem-Ilm-Chr)	Qz-Chl-Serp	0.41	0.01	528	196	384	7.0	0.7	0.0
VI24	semi-massive	Py-Cp-(Po-Sph-Hem-Mgt)	Qz-Chl	3.10	0.04	265	203	93	73	11	0.0
Type 4b) Stockwork veins in gabbro											
Campegli* (eastern Liguria)											
CP1	low-grade	Py-Cp-Sph	Qz-Alb-Chl	2.96	0.10	37	47	14	21	7.8	0.0
CP3	low-grade	Py-Cp-Sph	Qz-Alb-Chl	n.a.	n.a.	n.a.	n.a.	n.a.	n.a.	n.a.	n.a.
Type 4c) Stockwork veins in basalt											
Montecreto (central Emilia Romagna)											
MO11	high-grade	Py-Cp-(Po-Chr)	Qz-Cal-Chl-Serp	1.60	0.02	258	98	268	0.0	0.4	0.0
Boccassuolo (central Emilia Romagna)											
BO6	low-grade	Py-Cp-Sph	Qz-Cal-Chl	5.94	4.85	60	74	43	17	7.3	0.0
BO33	high-grade dissemi	Py-Cp-Sph	Qz-Cal-Chl	4.77	2.50	33	362	29	15	10.1	0.0
BO53	low-grade	Py-Cp-Sph	Qz-Cal-Chl	n.a.	n.a.	n.a.	n.a.	n.a.	n.a.	n.a.	n.a.
BO91	low-grade	Py-Cp-Sph-Gn-(Po)	Qz-Cal-Ep-Chl	n.a.	n.a.	n.a.	n.a.	n.a.	n.a.	n.a.	n.a.
BO93	low-grade	Py-Cp-Sph-Gn	Qz-Cal-Ep-Chl	n.a.	n.a.	n.a.	n.a.	n.a.	n.a.	n.a.	n.a.
BO96	low-grade	Py-Cp-Sph	Qz-Cal-Ep-Chl	n.a.	n.a.	n.a.	n.a.	n.a.	n.a.	n.a.	n.a.
BO97	low-grade	Py-Cp-Sph	Qz-Cal-Ep-Chl	n.a.	n.a.	n.a.	n.a.	n.a.	n.a.	n.a.	n.a.
BO98	low-grade	Py-Cp-Sph	Qz-Cal-Ep-Chl	n.a.	n.a.	n.a.	n.a.	n.a.	n.a.	n.a.	n.a.
Casali-Monte Loreto (eastern Liguria)											
CS5	low-grade dissemi	Py-Cp-Sph	Qz-Alb-Chl	1.61	0.04	50	260	13	0.0	0.7	0.0
Magmatic sulfide deposits emplaced in the ultramafic basement of the Ligurides before the Jurassic ocean-opening											
Stratiform ore concordantly emplaced in massive serpentinite											
Il Pozzo (Corchia, western Emilia Romagna)											
COPO1	massive	Py-Cp-Mgt-(Po-Pn-Sg-Mo-Sph)	Serp-Px-Hbl-Tlc-Chl-Dol	n.a.	n.a.	n.a.	n.a.	n.a.	n.a.	n.a.	n.a.
COPO2	massive	Py-Cp-Mgt-(Po-Pn-Sg-Mo-Sph)	Serp-Px-Hbl-Tlc-Chl-Dol	n.a.	n.a.	n.a.	n.a.	n.a.	n.a.	n.a.	n.a.
COPO3	massive	Py-Cp-Mgt-(Po-Pn-Sg-Mo-Sph)	Serp-Px-Hbl-Tlc-Chl-Dol	n.a.	n.a.	n.a.	n.a.	n.a.	n.a.	n.a.	n.a.
COPO4	massive	Py-Cp-Mgt-(Po-Pn-Sg-Mo-Sph)	Serp-Px-Hbl-Tlc-Chl-Dol	n.a.	n.a.	n.a.	n.a.	n.a.	n.a.	n.a.	n.a.

1) Total S wt% content of the ore: massive > 20%, semi-massive = 15-20%, stringers = 10-12%, high grade = 5-10%, low grade< 5%. 2) In brackets relevant accessory minerals.
Sulfides: Cp = chalcopyrite, Gn = galena, Mo = molybdenite, Po = pyrrhotite, Pn = pentlandite, Py = pyrite, Sg = siegenite, Sph = sphalerite; Oxides: Chr = chromite, Hem = hematite, Ilm = ilmenite, Mgt = magnetite; Silicates: Alb = albite, Chl = chlorite, Ep = epidote, Hbl = hornblende, Px = pyroxenes, Qz = quartz, Serp = serpentine, Tlc = talc; Carbonates: Cal = calcite, Dol = dolomite, Sid = siderite. 0.0 = below detection limit. n.a. = not analyzed.

(Garuti et al., 2008a). The analyzed samples (FE2, FE13) represent semi-massive and massive ore from a 25 cm-thick vein in the upper section of the serpentinite block. Here, the sedimentary mélange is absent, and the stockwork is abruptly cut by sub-horizontal layers of Palombini Shales, suggesting that the deposit was deeply eroded before deposition of the pelagic sediments (Garuti et al., 2008a). The Vigonzano mine comprises several stockwork deposits distributed in three serpentinite blocks surrounded by sedimentary mélange (Bertolani, 1959; Garuti et al., 2008a). Two samples (VI18, VI24) were collected from the main ore body of "Cantiere Vaie", where the stockwork veins may reach a thickness of more than 1 meter, and contain high-grade to semi-massive sulfide mineralization. One sample of massive sulfide (VI13) was collected in a small exploration gallery at Rocca Lagona, possibly representing the marginal zone of the stockwork.

Type 4b: One stockwork vein deposit hosted in gabbro was studied at Campegli (eastern Liguria, Fig 1A). Two samples showing low-grade dissemination of sulfide (CP1, CP3) were collected in a small assay gallery cutting across a vertical swarm of quartz veins up to some ten centimeters in thickness (Garuti et al., 2008a).

Type 4c: Three stockwork deposits hosted in pillow basalt were sampled in the old mines of Boccassuolo (BO6, BO33, BO53, BO91, BO93, BO96, BO97, BO98) and Montecreto (MO11) (central Emilia Romagna, Fig. 1C) and Casali-Monte Loreto (CS5) (eastern Liguria, Fig. 1A). The

stockwork deposits of Boccassuolo and Casali-Monte Loreto consist of a dense reticulate of quartz-calcite-chlorite-sulfide veins, up to more than one meter in thickness, emplaced in a hydrothermally altered pillow basalt and basalt breccia (Fig. 3E). The Montecreto sulfide deposit is hosted in hydraulic breccia composed of cm- to dm-sized fragments of spilitic basalt, mineralized veins and serpentinite, cemented by quartz, calcite and sulfide, and is believed to have formed by repeated cycles of hydraulic fracturing and ore-gangue deposition (Garuti et al., 2008a).

Magmatic sulfide in serpentinite: Four samples of magmatic sulfide (COPO1, COPO2, COPO3, COPO4) were collected in the copper mine "Il Pozzo" (Corchia ophiolite). This deposit has been described by Garuti et al. (2008b) and pertains to a group of Fe-Cu-(Ni) sulfide ores emplaced in the ultramafic basement of the Ligurides before the Jurassic ocean-opening (i.e., Monte Rossola, Monte Ramazzo ores). According to Ferrario (1977) and Ferrario and Garuti (1980) the sulfide ore originally formed by liquid immiscibility at magmatic temperatures, and subsequently underwent partial hydration-oxidation under regional and/or oceanic metamorphic conditions.

Controls on mineralogical and textural variations

According to Garuti and Zaccarini (2005) and Zaccarini and Garuti (2008), mineralogy, composition and texture of the sulfide ores have been influenced by the depositional en-

Table 3 - Representative analyses of major sulfide minerals in the investigated VMS deposits of the Northern Appennines ophiolites.

	n°	Fe	Ni	Co	Cu	Zn	Cd	Mn	S	As	Sum	Ni ppm	Co ppm
Detection Limit[1]		0.07	0.04	0.04	0.02	0.02	0.05	0.02	0.05	0.04			
Pyrite[2]													
BD6	6	47.15	0.06	0.03	0.20	0.00	na	0.00	52.56	0.05	100.05	588	342
BD8	16	47.53	0.10	0.06	0.08	0.03	na	0.02	52.19	0.18	100.19	1007	559
BDX	18	46.65	0.10	0.06	0.04	0.06	na	0.02	53.05	0.11	100.09	986	615
RP1	6	47.41	0.21	0.40	0.03	0.00	na	0.00	51.98	0.00	100.03	2080	4024
RP2	16	46.74	0.09	0.16	0.03	0.00	na	0.00	53.06	0.00	100.08	891	1569
CO1	22	45.71	0.26	0.71	0.24	0.05	na	0.00	52.55	0.09	99.61	2584	7092
CO8*	12	46.95	0.09	0.47		0.17	na	0.00	52.65	0.00	100.33	908	4679
CO12	10	47.10	0.16	0.21	0.11	0.08	na	0.00	52.39	0.04	100.09	1578	2117
CO17*	8	46.56	0.08	0.09		0.35	na	0.05	52.92	0.05	100.10	810	871
RP12	8	47.22	0.13	0.21	0.02	0.00	na	0.00	52.71	0.03	100.32	1322	2098
RP14	35	46.81	0.04	0.11	0.05	0.02	na	0.03	52.83	0.08	99.97	388	1129
LB12	7	46.72	0.04	0.09	0.04	0.03	na	0.00	52.91	0.18	100.01	364	899
LB13*	8	46.10	0.06	0.12	0.23	0.07	na	0.05	53.23	0.07	99.93	620	1232
FE2	8	46.10	0.08	0.06	0.00	0.00	na	0.00	53.85	0.00	100.09	779	632
FE13	13	46.72	0.37	0.24	0.31	0.04	na	0.04	52.23	0.06	100.01	3668	2365
VI13	5	46.50	0.09	0.07	0.00	0.00	na	0.00	53.27	0.02	99.95	914	713
VI18	5	46.68	0.07	0.07	0.00	0.00	na	0.00	53.17	0.02	100.01	733	662
VI24	12	46.37	0.10	0.08	0.02	0.02	na	0.01	53.27	0.08	99.95	980	802
CP1	21	46.30	0.12	0.16	0.16	0.07	na	0.03	52.93	0.08	99.85	1186	1562
CP3	5	47.15	0.16	0.24	0.00	0.03	na	0.00	52.51	0.00	100.09	1590	2366
MO11	7	46.37	0.44	0.05	0.00	0.00	na	0.00	53.27	0.00	100.13	4405	481
BO6	6	46.68	0.05	0.05	0.06	0.04	na	0.00	53.16	0.00	100.04	476	521
BO33	6	46.85	0.08	0.08	0.06	0.09	na	0.00	52.90	0.00	100.06	806	841
BO53	6	46.86	0.04	0.06	0.12	0.00	na	0.00	53.04	0.00	100.12	351	583
BO91	15	47.53	0.03	0.08	0.05	0.12	na	0.04	52.09	0.05	99.99	348	769
BO93	10	46.52	0.02	0.04	0.05	0.25	na	0.06	52.92	0.15	100.01	234	363
BO96	12	46.50	0.07	0.08	0.00	0.07	na	0.04	53.21	0.09	100.06	700	840
BO97	10	46.60	0.05	0.09	0.00	0.03	na	0.00	53.17	0.06	100.00	543	886
BO98	13	46.57	0.06	0.09	0.02	0.02	na	0.00	53.17	0.40	100.33	579	940
CS5	5	46.80	0.03	0.08	0.00	0.00	na	0.00	54.88	0.02	101.81	289	783
Pyrrhotite													
BD6	7	60.15	0.09	0.15	0.23	0.11	na	0.10	39.35		100.18	943	1477
BD8	6	60.43	0.16	0.04	0.14	0.16	na	0.00	39.20	0.08	100.21	1650	399
RP1	4	60.30	0.52	0.05	0.00		na	0.00	39.07	0.09	100.03	5229	502
RP2	11	60.83	0.09	0.09	0.00	0.07	na	0.17	38.97	0.31	100.53	877	881
LB12	10	56.91	0.06	0.04	0.00	0.00	na	0.14	42.93	0.31	100.39	561	386
VI18	5	61.20	0.09	0.04	0.59	0.00	na	0.00	38.55	0.10	100.57	916	378
FE2	8	59.61	0.19	0.06	0.52	0.00	na	0.00	39.86	0.11	100.35	1885	616
BO53*	2	60.02	0.04	0.07	0.00	0.18	na	0.00	39.89	0.00	100.20	385	653
BO91*	2	60.24	0.04	0.10	0.00	0.00	na	0.00	39.49	0.00	99.87	448	978
CO8*	7	58.56	0.16	0.36	0.00	2.44	na	0.00	38.47	0.23	100.22	1569	3556
Sphalerite													
BDX	9	4.06	0.06	0.00	2.28	59.63	0.13	0.16	34.17	0.22	100.71	588	0.00
CO1	8	5.10	0.05	0.08	5.18	56.30	0.00	0.00	33.28	0.03	100.02	475	793
CO8	38	11.10	0.19	0.27	1.25	54.65	0.12	0.00	33.30	0.10	100.98	1871	2695
CO17	13	10.44	0.12	0.22	1.05	55.29	0.12	0.15	33.42	0.36	101.17	1189	2196
LB13	14	2.15	0.04	0.00	1.44	62.06	0.07	0.10	34.11	0.24	100.21	321	0.00
FE13*	4	8.23	0.04	0.02	5.95	53.00	0.15	0.00	32.50	0.92	100.81	399	167
VI24*	26	5.19	0.04	0.08	1.53	59.50	0.24	0.12	33.52	0.27	100.49	409	761
CP1	16	4.84	0.05	0.03	1.12	60.17	0.19	0.18	33.60	0.31	100.49	455	309
CP3	13	4.29	0.05	0.04	1.12	61.83	0.19	0.18	33.11	0.27	101.08	504	378
BO6	5	7.05	0.09	0.00	8.11	50.97	0.10	0.12	33.59	0.33	100.36	909	0.00
BO33	8	5.98	0.03	0.00	2.51	58.14	0.16	0.20	33.12	0.33	100.47	278	0.00
BO53	21	5.30	0.08	0.00	6.23	54.87	0.00	0.00	33.57	0.00	100.05	783	0.00
BO91	12	7.84	0.05	0.00	8.69	50.21	0.18	0.13	33.17	0.19	100.46	491	0.00
BO93	7	6.42	0.03	0.00	7.29	53.16	0.06	0.08	32.93	0.28	100.25	279	0.00
BO96	10	1.31	0.04	0.00	0.18	65.43	0.24	0.20	32.72	0.27	100.39	393	0.00
BO97	16	1.31	0.04	0.00	0.30	65.47	0.15	0.19	32.67	0.36	100.49	403	0.00
BO98	8	1.37	0.05	0.00	0.16	65.67	0.16	0.19	32.64	0.25	100.49	493	0.00
Pyrite from magmatic sulfide deposits													
COPO1	5	46.14	0.12	0.06	0.00	0.00	na	0.00	53.66	0.00	99.98	1235	557
COPO2	15	46.23	0.15	0.05	0.00	0.09	na	0.00	53.44	0.00	99.96	1484	501
COPO3	9	46.16	0.12	0.06	0.00	0.00	na	0.00	53.62	0.00	99.96	1209	633
COPO4	12	46.18	0.22	0.11	0.00	0.13	na	0.00	53.18	0.00	99.82	2192	1070

n° = number of analyzed grains. Concentrations in wt%, except Ni and Co that are given also in ppm. 0.00 = below detection ninit. na = not analyzed. [1] Average detection limit. [2] Analysis of grain cores, except pyrite inclusions in other sulfides marked (*).
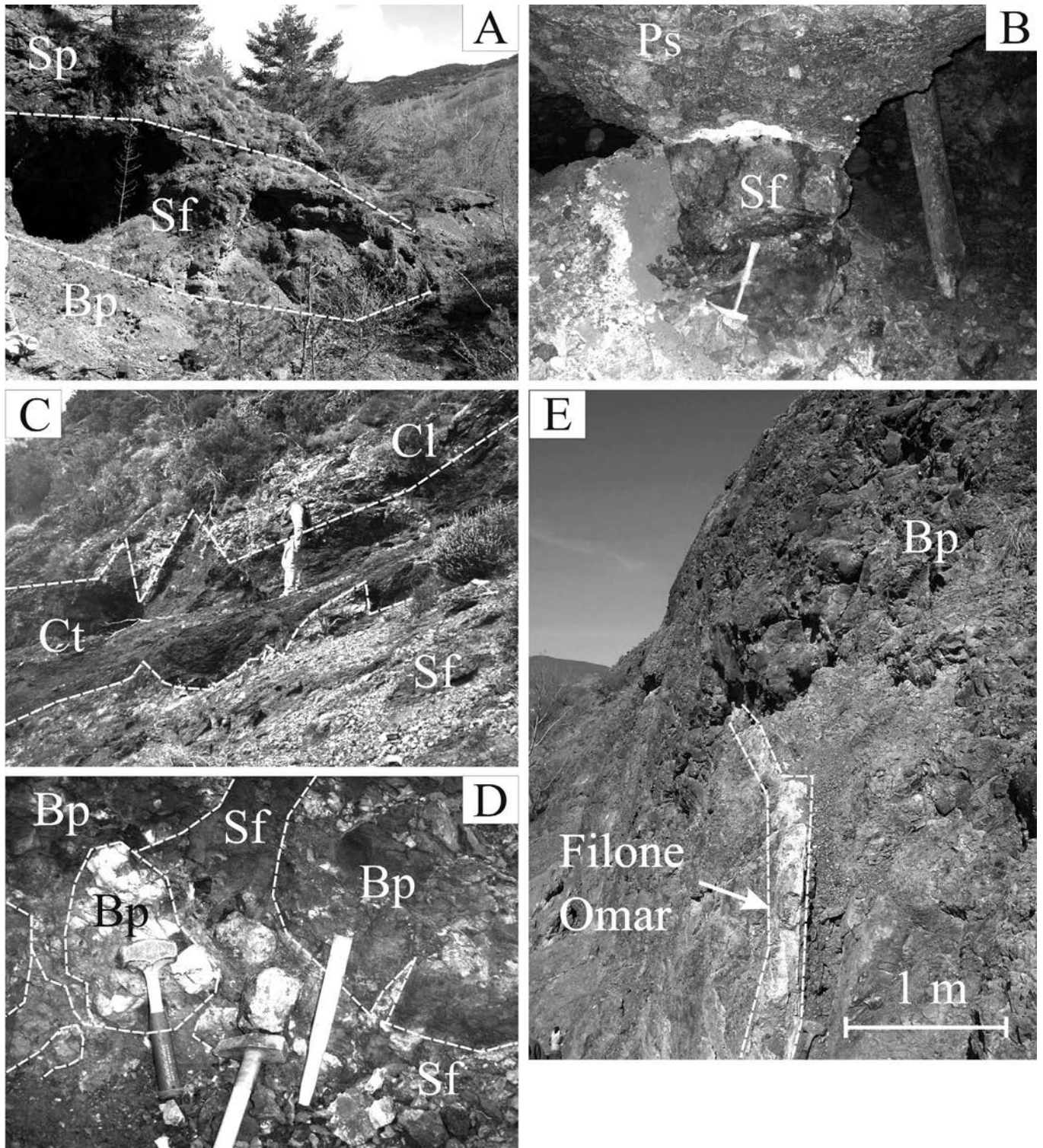
Fig. 3 - Field view of different types of VMS deposits in the Northern Apennine. A) Upper mining works in the Monte Bardeneto mine (alt., 778 m). Note that the stratigraphy is overturned. Sf- massive sulfide, Bp- pillow basalt, Sp- serpentinite breccia. B) Underground view of the Corchia mine (Cantiere Donnini). The massive sulfide (Sf) is covered by a Palombini Shales olistostrome (Ps). C) External outcrop of the Reppia II deposit showing the massive sulfide (Sf) covered by chert (Ct) and Calpionella Limestones (Cl). D) Massive sulfide network (Sf) infiltrating the pillow basalt (Bp), Libiola mine (external outcrop). E) View of the "Filone Omar", a vertically emplaced dike into pillow basalts (Boccassuolo).

vironment (seafloor vs. sub-seafloor) and country rock type (ultramafic vs. mafic).

Seafloor vs. sub-seafloor environment

Both stratiform and stratabound sulfide ores deposited at the seafloor are characterized by systematic anomalies in Au and U (Table 2). This feature has been interpreted as due to the interaction between the sulfide ore and fresh sea-water in submarine conditions (Garuti and Zaccarini, 2005 and reference therein). The two types of deposits, however, display differences in the sulfide texture. In contrast to the basalt stratabound deposit of Libiola, which was quickly

overwhelmed by the accumulating pillow lavas, the stratiform sulfides underwent long-lasting exposure at the seafloor that caused development of distinctive textures typical of a sedimentary environment (Ferrario and Garuti, 1980; Garuti and Zaccarini, 2005). Pyrite framboids are common and almost ubiquitous in all stratiform deposits (Fig. 4) but rare in the stratabound one. Other biogenic textures are exclusively found in stratiform deposits. Remnants of microfossil shells (mainly foraminifera and radiolaria) replaced by sulfides were observed at Corchia, and Reppia II (Fig. 5A to D). Sample CO1 from Corchia consists of resedimented detrital sulfide accumulated by debris-flows into topographic depressions of the seafloor, topped by a Palombini Shales olistostrome (Fig. 3B). The sulfide ore has been transformed into a massive, poorly-sorted clastic sediment, consisting of fragments of hydrothermal sulfides (pyrite, chalcopyrite, sphalerite) and abundant biologic remains embedded in a sandy matrix of quartz, chlorite and clay minerals (Fig. 5A, B). A variety of enigmatic structures were attributed to the activity of bacteria (Garuti and Zaccarini, 2005). At Monte Bardeneto, they may simply appear as vermiculations, stalks and filaments of sulfide (mainly pyrite) intimately intergrown with calcite and chlorite in the gangue rich portions of the massive ores (Fig. 6A). Corona-like structures are also frequent, varying in shape from rounded spherules to rod-like, rectangular or less regular aggregates. They consist of chains of minute pyrite euhedra enclosing a fine aggregate of Fe-Al-Mg silicate (Fe-rich chlorite or clay-like phase) intermixed with Fe-sulfide (Fig. 6B, C, D). Peculiar spheroids, up to 100-200 μm in size, have been described by Garuti and Zaccarini (2005) in the massive sphalerite ore of Corchia (samples CO8, CO17). They usually occur in closely packed assemblages forming either botryoidal aggregates of sphalerite-silica spheroids coated with a thin film of silica or a concentric, palisade-like array of sphalerite crystallites (Fig.7). Magnetite spherules of about 30-100 μm have been observed in sample BD8 from Monte Bardeneto. They appear as complete or incomplete rings with jagged or scalloped outlines, surrounding a core of Fe-Al-Mg silicate, possibly Fe-rich chlorite. The spherules are attached to the external border of large sulfide aggregates or occur isolated in the calcite matrix (Fig. 8A, B). The spherules concentrate in magnetite-rich domains in which magnetite also occurs either as small (< 300 μm) lozenge-shaped idiomorphic crystals within the calcite matrix (Fig. 8C) or a large aggregates associated with the primary hydrothermal assemblage pyrrhotite-chalcopyrite-pyrite (Fig. 8D). Rare hematite has been observed in the calcite matrix or as inclusions in magnetite.

The stockwork sulfides precipitated from hydrothermal fluids flowing upwards along fractures and cracks in the rock substrate. Some deposits (i.e., Boccassuolo, Casali-Monte Loreto, Ferriere) extend over a vertical distance of several hundreds of meters, suggesting that ore deposition started at relevant depth below the seafloor (Garuti et al., 2008a). The sulfide texture indicates crystallization and grain coarsening with development of straight grain boundaries and idiomorphic crystal shapes. There is no evidence of biologic replacement or sedimentary reworking. The lack of contact with fresh seawater in the sedimentary environment has not produced Au and U anomalies (Garuti and Zaccarini, 2005). Only sample FE13 exhibits some enrichment in Au and U (Table 2) suggesting a possible influence of fresh seawater during seafloor erosion of the stockwork at

Ferriere (Garuti et al., 2008a).

Application of the chlorite geothermometer (Kranidiotis and MacLean, 1987) to 645 chlorite grains from 64 samples
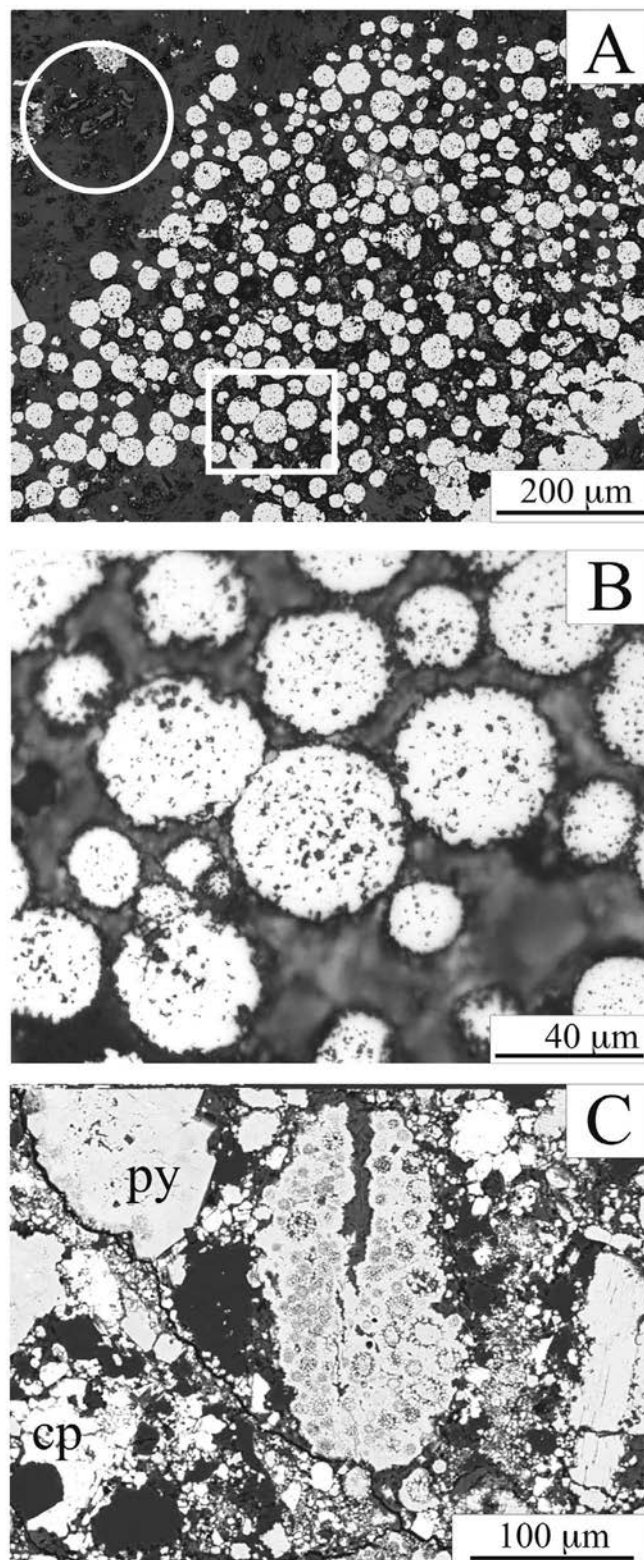

Fig. 4 - A) Pyrite framboids from Monte Bardeneto. Note the skeletal crystal of chromite partially replaced by chlorite, included in calcite (white circle). B) Detail of the microphotograph in A (white box) showing the chlorite matrix interstitial to the framboids. C) Large fragment of pyrite with framboidal texture in accumulated sulfide debris of Corchia (sample CO1); py- pyrite, cp- chalcopyrite, dark grey- quartz, chlorite and clay minerals. A) and B) reflected light images; C) BSE image.
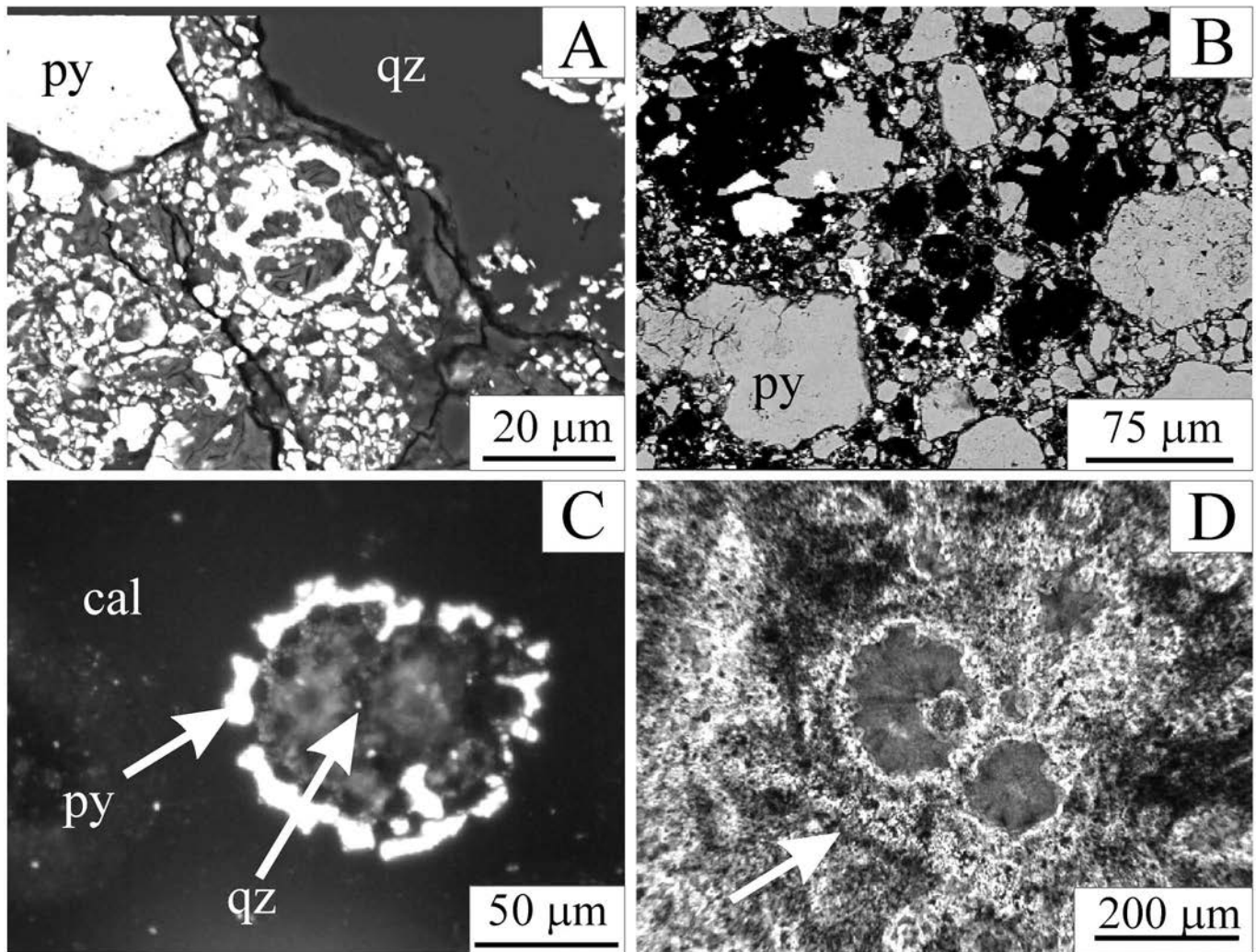
Fig. 5 - Remnants of foraminifera and radiolaria from seafloor stratiform VMS deposits of the Northern Apennine ophiolites. A) and B) Shells of foraminifera replaced by pyrite and chalcopyrite in accumulated sulfide debris of Corchia (sample CO1). Note the chlorite filling of the fossil shells (BSE images); C) Radiolarian shell replaced by pyrite included in the calcite matrix of sample RP12 from yhe Reppia II deposit (reflected light). D) Radiolarian shells and spiculae (arrow) from a radiolarite layer of the sedimentary cover at Montecreto (transmitted light). qz- quartz, cal- calcite, other abbreviations as in Fig. 4.

gave results consistent with the inferred environments of sulfide deposition (Zaccarini et al., 2003; Zaccarini and Garuti, 2008). High temperatures from 200°C to 360°C (av., 255°C) were obtained for the stockwork and stratabound ores. They mark the thermal range of hydrothermal fluids uprising through the sub-seafloor or emanating from extruding basalt. In contrast, chlorite from seafloor stratiform ores gave an average temperature of 170°C, with 85% of the data points between 50°C and 200°C. Most of these chlorites display interlayering with clay-type sheet silicates possibly caused by submarine weathering during long-time exposure at the seafloor (Zaccarini and Garuti, 2008). Significantly, the chlorite temperatures obtained for the seafloor stratiform deposits are similar to those deduced from O isotopes (< 200°C) in igneous rocks far from the veins, which were interpreted to indicate prolonged reaction with relatively cold seawater at or near the seafloor (Barrett and Friedrichson, 1989).

Influence of the host rock lithology

Compared with the sulfide ores hosted in mafic rocks (basalt and gabbro) those associated with serpentinite and serpentinite breccia (types 1 and 4a) are characterized by the common occurrence of pyrrhotite, scarcity of sphalerite, high Cu/Zn and Ni/Co ratios in both the bulk ore and in individual pyrite grains. They also are enriched in total Cr, due to the presence of chromite and clinochlore characterized by high Cr/Mn, Mg/Fe, and Mg/Al ratios (Zaccarini and Garuti, 2008). Field relations show that these deposits formed before a significant outflow of basaltic lava (Garuti et al., 2008a), therefore the hydrothermal fluids interacted mainly with the mantle basement, resulting preferentially enriched in compatible elements with strong ultramafic affinity (Ni, Mg, Cr). Hydrothermal leaching and rock-fluid metasomatic reactions were the active chemical mechanisms. However, the sulfide ore was also enriched in the compatible elements by mechanical incorporation of detrital ultramafic minerals (i.e., chromite, serpentine) and ultramafic rock fragments liberated in situ, or transported from the substrate. Evidence for transport of ultramafic-derived material over long distances is observed in the stockwork deposit at Montecreto. Here, the sulfide ore is hosted in a hydraulic breccia intruding the pillow basalt unit. Both the breccia and the sulfide ore contain abundant fragments of chromitite and serpentinite eroded from the underlying ultramafic substrate, and transported upwards during explo-
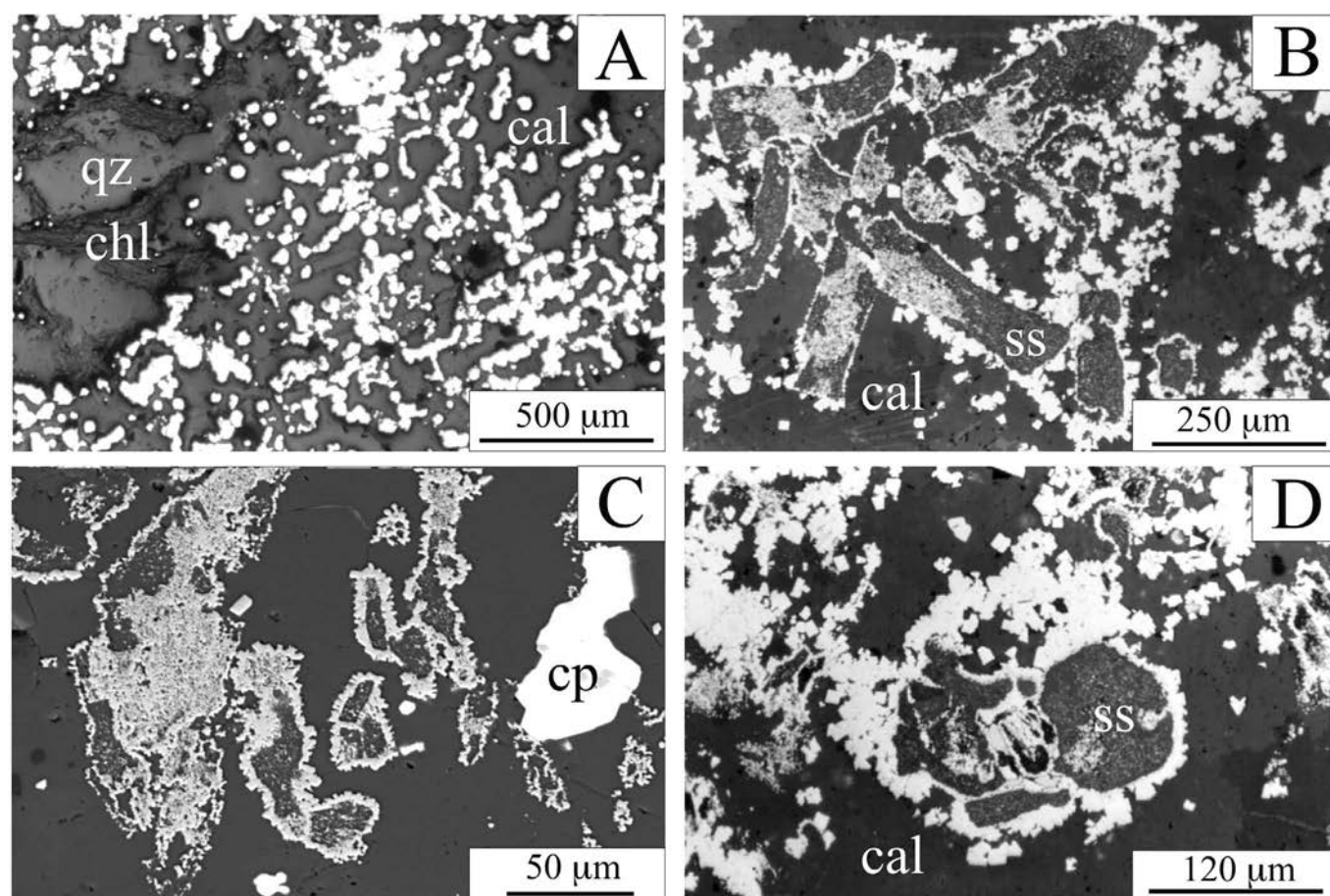
Fig. 6 – Biogenic ore textures in the seafloor stratiform VMS deposit of Monte Bardeneto interpreted as sulfides and sulfide-silicate minerals nucleated on bacterial cells. A) Pyrite vermiculations, stalks, and filaments in calcite matrix; note the large aggregate of quartz and chlorite on the left side (sample BDX). B) Chains of pyrite euhedra surrounding intermixed (Fe-Al)-silicate and sulfide in calcite matrix (sample BD6). C) Same as in B) but in quartz-calcite matrix; the white grain is chalcopyrite (sample BD6). D) Same as in B) and C) in calcite matrix (sample BD8). A), B) and D) reflected light images; C) BSE image. ss- (Fe-Al)-silicate and sulfide, other abbreviations as in Figs. 4 and 5.

sive emplacement. Because of the interaction with the ultramafic substrate, the Montecreto deposit displays the compositional characters of the serpentinite-hosted deposits. The gabbro-hosted sulfide veins (Campegli) have composition similar to those of basalt-hosted deposits.

Magmatic sulfides in serpentinite

The mineralogy of the Fe-Cu-Ni magmatic sulfides is characterized by pyrite, chalcopyrite, magnetite and siegenite, with accessory sphalerite, molybdenite and gold. Gangue minerals are pyroxenes, serpentine, talc, chlorite and dolomite, whereas quartz, ubiquitous in the gangue of the hydrothermal deposits, is conspicuously absent (Garuti et al., 2008b). Textural evidence clearly indicates that magnetite and siegenite are secondary phases after the primary sulfides pyrite, chalcopyrite and pentlandite.

SULFIDE MINERAL CHEMISTRY

Electron microprobe compositions of sulfide minerals in the investigated samples (Table 3) are consistent with the data reported in the previous works (Ferrario and Garuti, 1980; Garuti and Zaccarini, 2005; Zaccarini and Garuti, 2008). The composition of chalcopyrite reflects the stoichiometry $CuFeS_2$ without detectable substitutions. Pyrite

displays variable contents of Ni (234 - 4405 ppm) and Co (342 - 4679 ppm). Both metals are enriched in the cores of grains, with the exception of tiny pirite inclusions in sphalerite and chalcopyrite that are homogeneous. The Co/Ni ratio of pyrite varies from 0.11 to 1.93 (av., 0.87) in ultramafic-hosted deposits, and from 1.04 to 5.15 (av., 1.99) in deposits associated with basalt. The Ni and Co contents of pyrite from magmatic sulfide deposits in serpentinite vary in the ranges 1209-1484 ppm and 501-1070 ppm, respectively, with Co/Ni ratios from 0.34 to 0.52 (av., 0.45), lower than those from pyrite in ultramafic-hosted hydrothermal ores. Pyrrhotite is the monoclinic variety (Fe_7S_8) and may contain significant amounts of Ni (385-5229 ppm) and Co (378-3556 ppm). The Co/Ni ratio varies from 0.10 to 1.57 (av., 0.61) in coarse pyrrhotite from ultramafic-hosted deposits, but is as high as 2.27 (av., 1.71) in small pyrrhotites included in pyrite and sphalerite from the basalt-hosted ores of Boccassuolo and Corchia. Sphalerite contains significant amounts of iron and copper up to 11.1 wt% Fe and 8.7 wt% Cu, respectively. With the exception of the massive sphalerite from Corchia, that is iron rich (11.1 wt% Fe) and copper poor (1.25 wt% Cu), in most cases, Fe and Cu correlate positively according to regression lines parallel to the Cu/Fe ratio of chalcopyrite (Fig. 9). This feature is considered as an analytical artifact due to the "chalcopyrite-disease" texture of sphalerite.
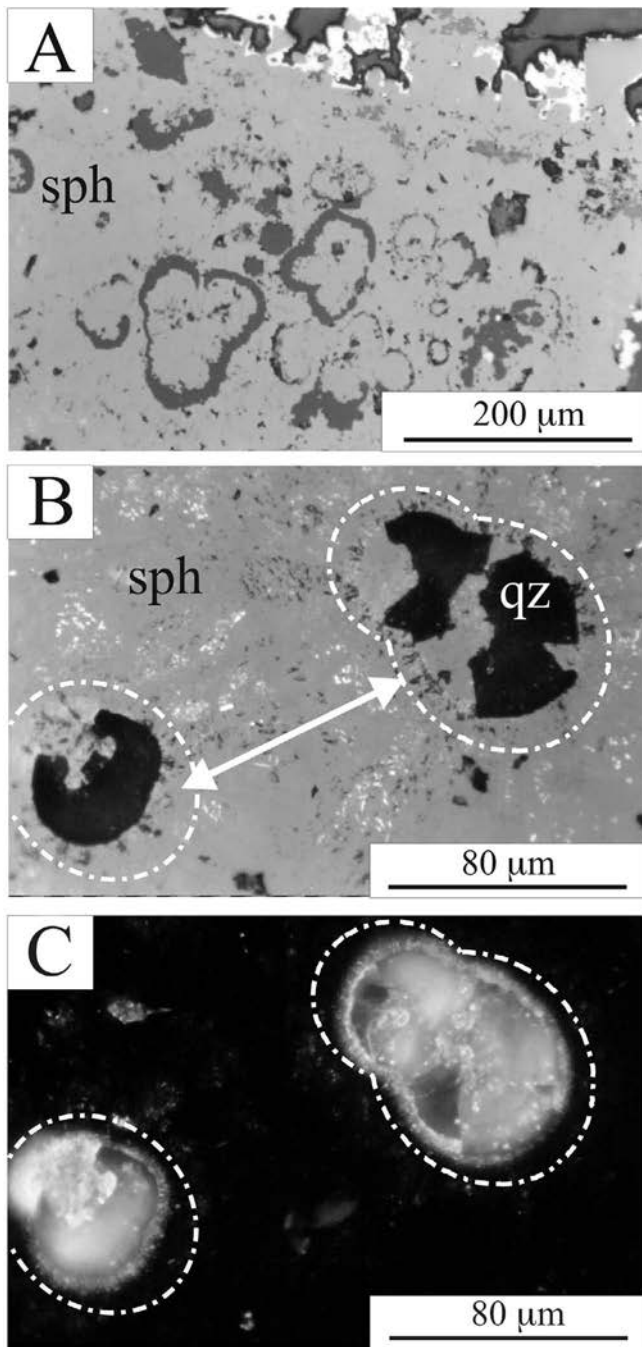
Fig. 7 - Biogenic textures in massive sphalerite in sample CO8 from the seafloor stratiform VMS deposit of Corchia (reflected light). A) Botryoidal aggregates of sphalerite-silica spheroids interpreted as minerals nucleated on bacterial cells; white crystals on top and right side are pyrite replacing sphalerite. B) Individual spheroids including silica (qz) in sphalerite; the arrow indicates the concentric, palisade-like crystallites of sphalerite bordering the spherulae. C) Same as B) under crossed Nichols; note that sphalerite intergrown with silica at the core of spherulae has intense internal reflections, in contrast with the deep extinction of the sphalerite matrix. sph- sphalerite.

RESULTS OF SULFUR ISOTOPE ANALYSIS

The whole data set of $\delta^{34}S$ obtained for the Northern Apennine VMS deposits (Table 4) ranges between -2.9‰ and +11.4‰ (av., +5.9‰), besides just one anomalous value of +22.8‰ in sample RP2B. The $\delta^{34}S$ vary from -0.6‰ to +11.3‰ in pyrite (av., +5.2‰), -2.9‰ to +11.4‰ in chalcopyrite (av., +6.7‰), and 0.0‰ to +10.3‰ in spha-

lerite (av., +6.1‰) (Fig. 10A). Two pyrrhotite grains from Monte Bardeneto and Reppia I gave $\delta^{34}S$ values of 3.0‰ and 6.2‰, respectively. Significant differences are observed among deposits when they are sorted by structural type (Fig. 10B). Stockwork veins hosted in gabbro (Campegli) and basalt (Boccassuolo, Casali-Monte Loreto) have very similar average $\delta^{34}S$‰, of +8.7‰ and +8.9‰, respectively. A comparable average value of +7.9‰ is found in the basalt-stratabound deposit of Libiola. Stockwork veins hosted in serpentinite (including Montecreto) have a significantly lower average $\delta^{34}S$ = +5.8‰. The stratiform deposits have the lowest $\delta^{34}S$, showing no difference between deposits hosted in serpentinite (av., +2.4‰) and basalt breccia (+2.5‰). They also display negative $\delta^{34}S$ values down to -2.3‰ and -2.9‰ in samples BD8 and CO1, from Monte Bardeneto and Corchia, respectively. The $\delta^{34}S$ values for magmatic sulfides in serpentinite vary from 0.0‰ to +2.8‰ in pyrite, with only one negative value of -1.7‰ from pyrite in sample COPO2, and +0.5‰ to +1.0‰ in chalcopyrite, with a total average of +0.7‰, calculated for 15 measurements.

DISCUSSION

Source of metals and sulfur in Phanerozoic VMS deposits

The first observation of "black smokers" at the axis of the East Pacific Rise, near 21°N and 109°W, provided unequivocal evidence for the massive deposition of sulfides from hot, metal-charged solutions venting onto the ocean floor (Francheteau et al., 1979). This historical discovery and the subsequent exploration of modern ocean-floor by the ocean drilling programs (see references in Goodfellow and Zierenberg, 1999) have provided invaluable insights into the nature of submarine hydrothermal activity, confirming the predicted hypothesis that ancient, on-land Volcanic-associated Massive Sulfides (VMS) were originally deposited from hydrothermal solutions at or below the seafloor. They generally occur within volcano-sedimentary sequences and show consistent space-time relationships with extrusive magmatic activity. A number of studies addressed to the identification of the primary source of metals and sulfur which are the major constituents of VMS deposits. Experimental data and the study of modern submarine hot-springs have demonstrated that the metal constituents are largely derived from leaching of foot-wall igneous rocks, with a possible contribution from the magmatic source responsible for volcanism (Reed, 1983; Lyndon, 1988; Seyfried et al., 1999). The model implies a long lasting convective circulation of hot solutions through the rock substrate, triggered by a heat source emplaced at shallow depth in the lithosphere, and requires continuous transfer of large volumes of water from an almost infinite reservoir to the hydrothermal system.

Considering the geologic setting of VMS deposits within ophiolite sequences, the obvious evidence is that fluids circulating in sub-oceanic hydrothermal cells must consist mainly of heated and chemically modified seawater, with possible contribution from the igneous source that provides heat for the convection. The broad, positive correlation between the sulfur isotopic compositions in Phanerozoic and modern VMS and coeval seawater sulfate (Fig. 11) supports the proposed genetic linkage between the mineralizing hydrothermal fluids and seawater (Sangster, 1968; Claypool et al., 1980). The average sulfide/sulfate fractionation factor
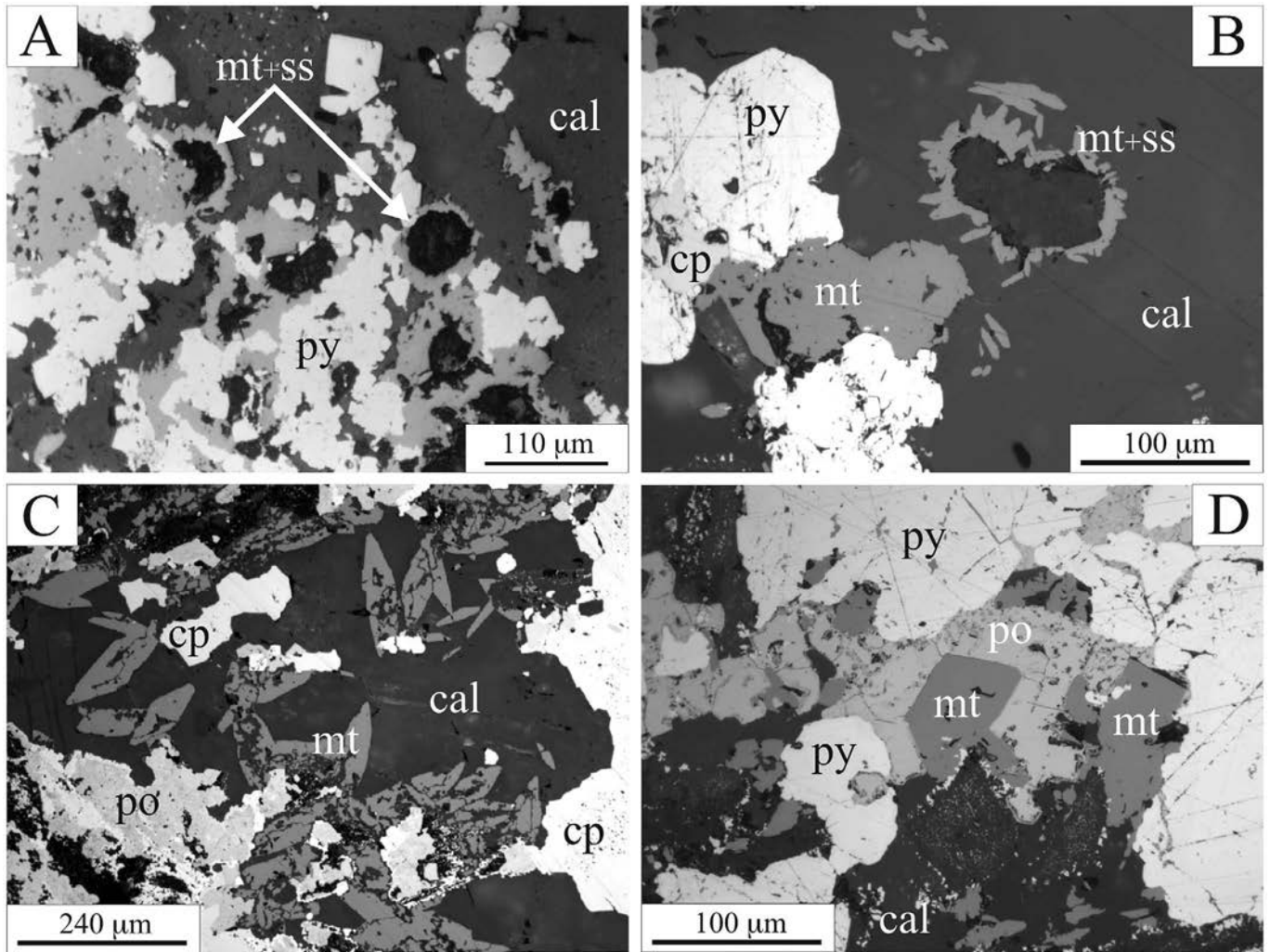
Fig. 8 - Magnetite spherulae in sample BD8 from the seafloor stratiform VMS deposit of Monte Bardeneto (reflected light). A) and B) Magnetite spherules with (Fe-Al)-silicate infilling (mt+ss) in calcite matrix. C) Cluster of lozenge-shaped magnetite (mt) associated with sulfides and calcite. D) Magnetite aggregates associated with primary sulfides. po- pyrrhotite; other abbreviations as in Figs. 4, 5 and 6.
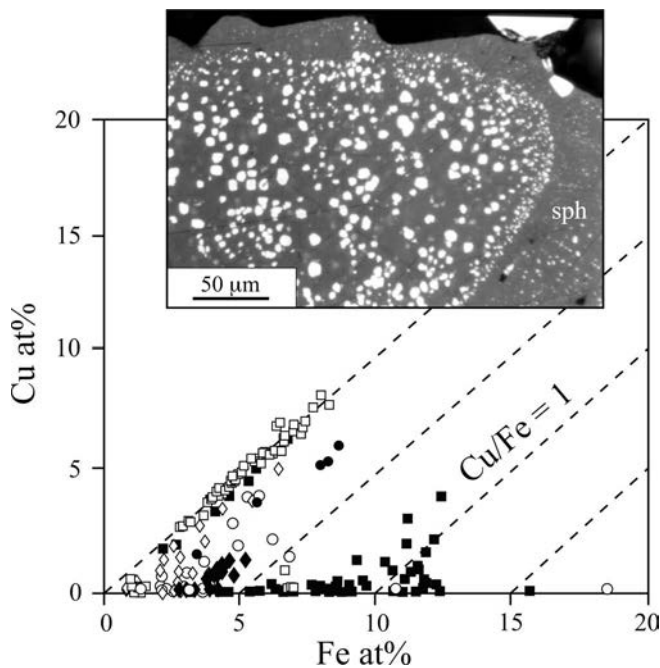
($\Delta_{H2S-SO4}$) is about -16.5‰ (Huston, 1999), implying remarkable reduction of sulfur in metal sulfides with respect to seawater sulfates. Proposed sources of reduced sulfur in VMS younger than 1.0 Ga include: i) partial to complete inorganic reduction of seawater sulfur during convective circulation in the rock substrate (Green et al., 1981; Ohmoto, 1986), ii) leaching of magmatic sulfides in the igneous rock substrate (Ohmoto, 1986; Solomon, 1976; Ohmoto and Goldhaber, 1997), iii) juvenile sulfur directly emanating from the same magmatic heat source that causes the convective circulation (Ohmoto and Goldhaber, 1997; Rye, 2005), iv) biogenic reduction of seawater sulfate (Sangster, 1968; Ohmoto and Goldhaber, 1997).

Data from the Northern Apennine VMS deposits have been plotted in the Age/δ^{34}S‰ covariation diagram (Fig. 11), by assuming a Late Jurassic age of 160 Ma. Convective

Fig. 9 - The "chalcopyrite-disease" texture (reflected light) causing spurious Fe and Cu contents in the electron microprobe analyses of sphalerite (sample BO6 from "Galleria Labirintica", Boccassuolo). The diagram shows the sharp positive correlation between Cu and Fe according to 1 : 1 regression lines, indicating that Cu and proportional amounts of Fe are due to mixed microprobe analysis of chalcopyrite inclusions. Open square-Boccassuolo, filled square- Corchia; open circle- Vigonzano; filled circle-Ferriere; open diamond- Libiola; filled diamond- Campegli.

Table 4 - Isotope data for VMS deposits of the Northern Appennines ophiolites.

Deposit Type / Locality / Sample	Isotope δ³⁴S‰				Total average
	Py	Cp	Sph	Po	
Hydrothermal Volcanic Massive Sulfides emplaced during Jurassic ocean opening					
Type 1) Stratiform ore in seafloor serpentinite breccia covered by pillow basalt					**2.4**
Monte Bardeneto (eastern Liguria)					
BD6	7.5	5.3		3.0	5.3
BD8	-0.6	-2.3			-1.5
BDX	0.6 , 1.2 [2]				0.8
Reppia I (eastern Liguria)					
RP1	1.9	0.7			1.3
RP2B	22.8 [3]			6.2	6.2
Type 2) Stratiform ore in seafloor basalt breccia covered by pelagic sediments					**2.5**
Corchia (western Emilia Romagna)					
CO1	0.9	-2.4 , -2.9 [2]	0.0		-1.1
CO12	3.3				3.3
CO8	4.4		4.9		4.7
CO17		5.8	5.3		5.6
Reppia II (eastern Liguria)					
RP12	5.4				5.4
RP14	3.1				3.1
Type 3) Stratabound deposits in pillow basalt					**7.9**
Libiola (eastern Liguria)					
LB12	6.6	9.5			8.0
LB13		8.4 , 8.9 [2]	6.0		7.8
Type 4a) Stockwork veins in serpentinite					**5.8** [4]
Ferriere (western Emilia Romagna)					
FE2	3.9				3.9
FE13	5.1	5.6			5.4
VI13	5.5				5.5
VI18	6.6				6.6
VI24	6.6	6.7			6.7
Type 4b) Stockwork veins in gabbro					**8.7**
Campegli (eastern Liguria)					
CP1		8.0			8.0
CP3	9.1	9.6			9.3
Type 4c) Stockwork veins in basalt					**8.9** [5]
Montecreto (central Emilia Romagna)					
MO11	6.2				6.2
Boccassuolo (central Emilia Romagna)					
BO6	9.7	10.0	4.0		7.9
BO33	7.9 , 11.3 [2]	11.1	9.6		10.0
BO53	10.7	11.4			11.1
BO91	4.5	9.5	10.3		8.1
BO93		10.9			10.9
BO96		7.4	7		7.2
BO97		7.7	7.9		7.8
BO98		7.5			7.5
Casali-Monte Loreto (eastern Liguria)					
CS5		10.7			10.7
Mineral average	**5.2**	**6.7**	**6.1**	**4.6**	
Magmatic sulfide deposits emplaced in the ultramafic basement of the Ligurides before the Jurassic ocean-opening					
Stratiform ore concordantly emplaced in massive serpentinite					**0.7**
Il Pozzo (Corchia, western Emilia Romagna)					
COPO1	0.0	0.7			0.4
COPO2	-1.7 , 0.2 , 0.7 [2]	0.7 , 1.0 [2]			0.3
COPO3	1.0 , 1.1 [2]	0.6			0.8
COPO4	1.3 , 2.8 [2]	0.5 , 0.9 [2]			1.4
Mineral Average	**0.7**	**0.7**			

1) average of all mineral data; 2) values from different grains; 3) value excluded from calculations; 4) includes the value from Montecreto; 5) the value from Montecreto excluded (see text for explanation). Sulfides: Py = pyrite; Cp = chalcopyrite; Sph = sphalerite; Po = pyrrhotite.

hydrothermal circulation through the rock substrate of the Ligurian Tethys might have covered a time span of about 30 Ma, between initial denudation of the peridotite-gabbro basement at the ocean floor (Early to Middle Jurassic) and the decline of volcanic activity, marked by widespread de-

position of pelagic sediments (Late Jurassic - Early Cretaceous). Therefore some serpentinite-hosted stockwork deposits (types 4a) may be quite old, dating back to the early stages of ocean opening (Garuti et al., 2008a). However, the close time relation between hydrothermal activity and
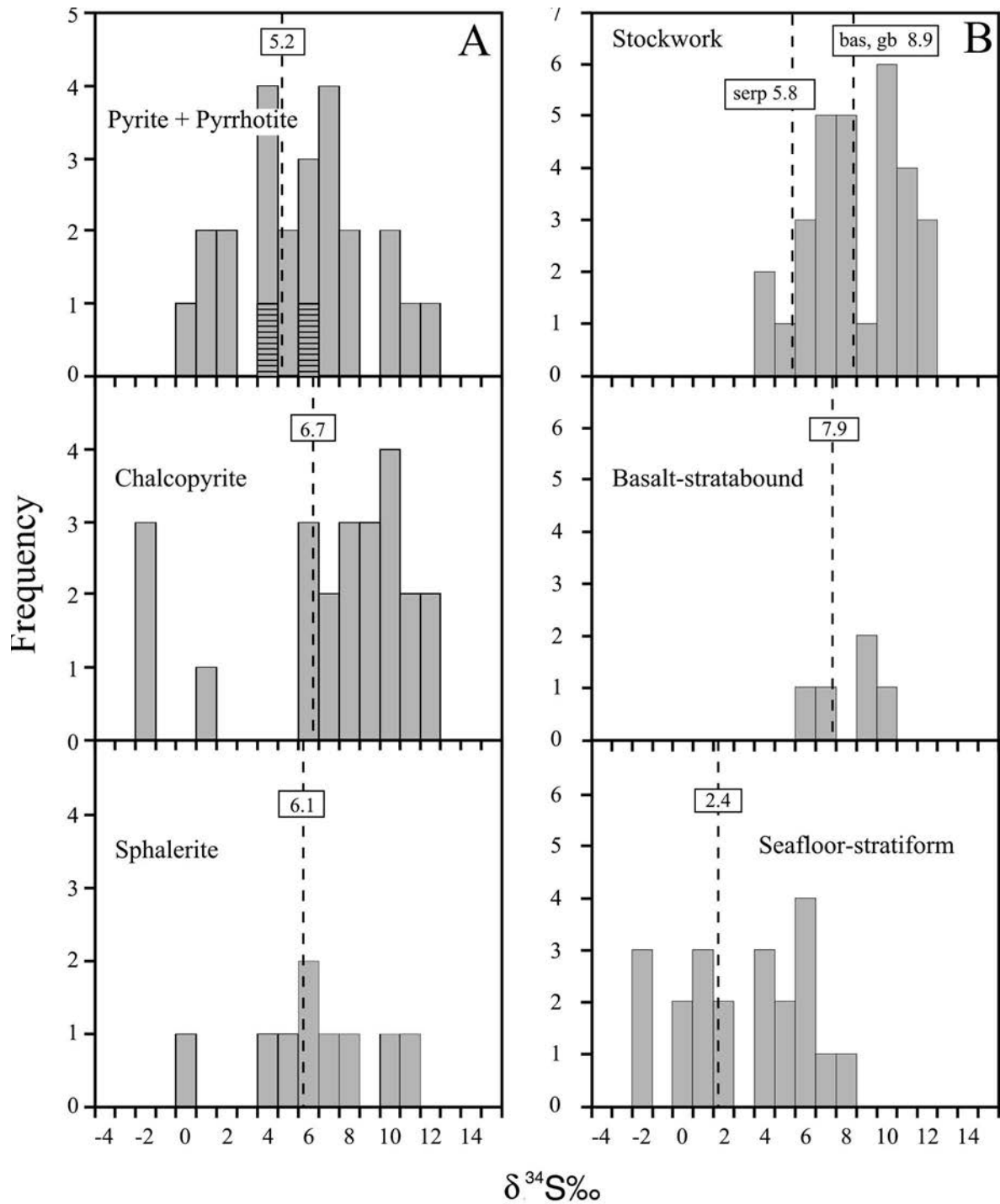
56

Fig. 10 —-Statistical variations of δ³⁴S‰ in VMS deposits of the Northern Apennine, A) sorted by sulfide mineral (dashed area-pyrrhotite), and B) sorted by structural type. Abbreviations: bas- basalt, gb- gabbro, serp- serpentinite. Average δ³⁴S‰ in frame.

basaltic magmatism would place the onset of the mineralizing episodes in the Late Jurassic, at about 160-150 Ma, as supported by dating of basalts and associated radiolarian cherts (Bortolotti et al., 1991; Marcucci and Passerini, 1991). The Northern Apennine VMS deposits have an average δ³⁴S of +5.9‰, comparable with data from Cretaceous (~ 80-95 Ma) VMS deposits in Tethyan ophiolites of Troodos and northeastern Turkey (Fig. 11). However, like many other Phanerozoic deposits, they show a great variability of

δ³⁴S, from +11.4‰ to negative values of the order of -2.9‰. In the Northern Apennine hydrothermal deposits, isotopic variations appear to be primarily controlled by the structural setting, indicating different trends for sulfide ores formed below or at the seafloor. In addition, the sub-seafloor deposits display differences attributable to the ultramafic vs. mafic nature of the country rock (Fig. 12). The possible sources of sulfur in the various types of deposits are discussed below.

Origin of sulfur in VMS deposits
of the Northern Apennine

Basalt-stratabound deposit: possible contribution of juvenile sulfur

The $\delta^{34}S$ values of mantle-derived mafic magmas are believed to be originally close to 0.0‰. Likewise, sulfides in igneous rocks are generally characterized by low $\delta^{34}S$ values, although deviations of 0.0‰ ± 5‰ are common (Ohmoto and Goldhaber, 1997). High temperature fluids emanating from magmas (> 400°C) contain gaseous SO_2 that generates both H_2S and SO_4^{2-} by hydrolysis during rapid cooling (Ohmoto and Goldhaber, 1997):

$$4SO_2 + 4H_2O \rightarrow H_2S + 6H^+ + 3SO_4^{2-}$$
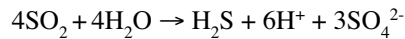
Daughter solid species of the reaction (sulfides and sulfates) exhibit fractionation factors $\Delta_{H2S-SO4}$ between -16‰ and -28‰. Therefore, given the initially low $\delta^{34}S$ values of magmatic sulfur, this inorganic reaction can produce sulfides with low and even negative $\delta^{34}S$ (Ohmoto and Goldhaber, 1997; Rye, 2005).

As to the Northern Apennine VMS, mixing with magmatic sulfur may have occurred in the case of the stratabound deposit of Libiola, where hydrothermal sulfides precipitated in close association with the extrusion of pillow-basalt (Ferrario and Garuti, 1980). The $\delta^{34}S$ values are comprised between +6.0‰ and +9.5‰ (av., = +7.9‰), implying a fractionation factor $\Delta_{H2S-SO4}$ of -9.5‰ with respect to coeval seawater sulfate at 160 Ma (~ +17.04 $\delta^{34}S‰$) (Fig. 11). The lack of biological-derived textures in the sulfide ore and the high temperature (> 250°C), well above the limit for the development of bacterial activity, suggest that reduced sulfur was not produced via organic reactions. Although we cannot provide any quantitative evidence, the isotopic composition of the stratabound sulfide might have resulted from a combination of different inorganic processes taking place in the various stages of ore formation: i) reduction of seawater sulfate and leaching of sulfide from the substrate basalt, during convective circulation before venting, ii) reduction of fresh seawater at the seafloor venting site, iii) addition of magmatic sulfur from degassing pillow basalt, during or after sulfide precipitation.

Stockwork veins: the role of country rock leaching

Reduction of the seawater SO_4^{2-} molecule took place during convective circulation through the rock substrate that led to formation of stockwork deposits. In general, it requires large amounts of H^+ that can be produced according to a variety of biological and no-biological reactions: i) non-bacterial, thermochemical reduction of sulfate by reaction with organic matter (thermochemical sulfate reduction); ii) bacterial-mediated decomposition of organic matter (biologic sulfate reduction), or iii) hydrothermal alteration of the country rocks (inorganic reduction) (Ohmoto and Goldhaber, 1997 and references therein). Reactions of type i) and ii) involving organic matter or bacteria are considered unlikely in the stockwork deposits of the Northern Apennine. In fact, they formed in the sub-seafloor, isolated from fresh seawater, in the apparent lack of any kind of organic matter or bacterial activity. There is no field evidence that the solutions cut across sedimentary horizons enriched in organic matter. Furthermore, the temperature estimates (200-350°C) extend significantly above the thermal range in which bacterial and non-bacterial decomposition of organic matter can take place (Ohmoto and Goldhaber, 1997). Thus reduction of the
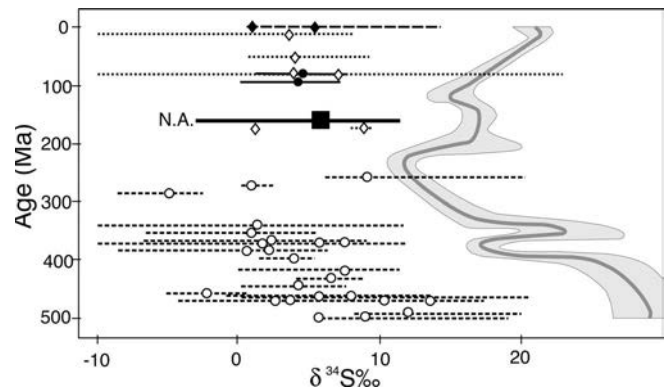

Fig. 11 - Evolution of $\delta^{34}S$ in Phanerozoic to Modern VMS deposits and coeval seawater sulfate. Symbols and lines indicate mean and ranges of variation of VMS deposits (data from Huston, 1999): black square- Northern Apennine (N.A); black diamonds- Red Sea and western Pacific; black dots- Tethyan VMS of Cyprus and northeastern Turkey; open diamonds- Mesozoic VMS; open circles- Paleozoic VMS. The heavy line and grey area indicate the evolution with age of the seawater-sulfate after Claypool et al. (1980).
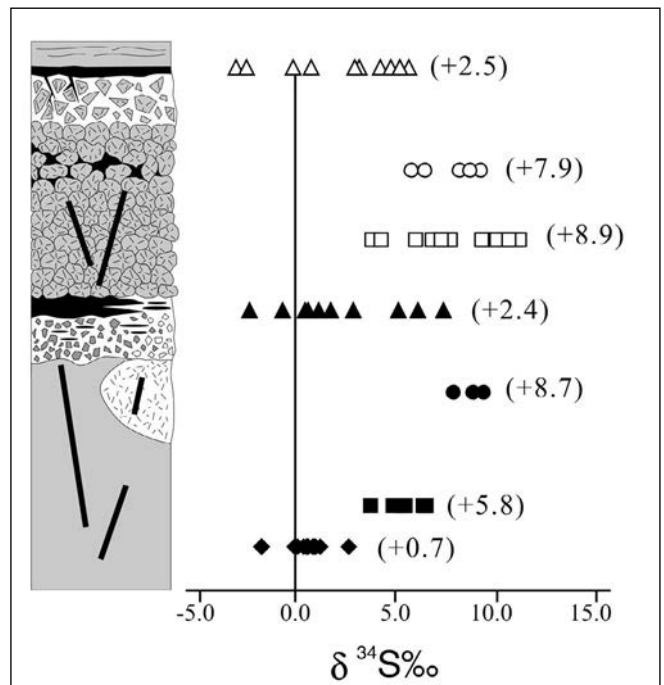

Fig. 12 - Variation of $\delta^{34}S$ ratios as function of the structural type of the Northern Apennine VMS deposits. Black squares- stockwork veins in serpentinite (Vigonzano, Ferriere); black dots- stockwork veins in gabbro (Campegli); black triangles- seafloor stratiform ore in serpentinite breccia (Monte Bardeneto, Reppia I); open squares- stockwork veins in basalt (Boccassuolo, Montecreto, Casali-Monte Loreto); open circles- stratabound ore in basalt (Libiola); open triangles- seafloor stratiform ore in basalt breccia (Corchia, Reppia II); black diamond- magmatic sulfide ore in serpentinite (Il Pozzo).

seawater sulfate was probably an essentially inorganic process.

Seawater penetrating at depth into the sub-seafloor of the Ligurian Ocean became progressively hotter and was chemically modified by reaction with mafic and ultramafic igneous rocks (Zaccarini and Garuti, 2008). Experimental studies on seawater/rock interaction indicate that mafic-ul-
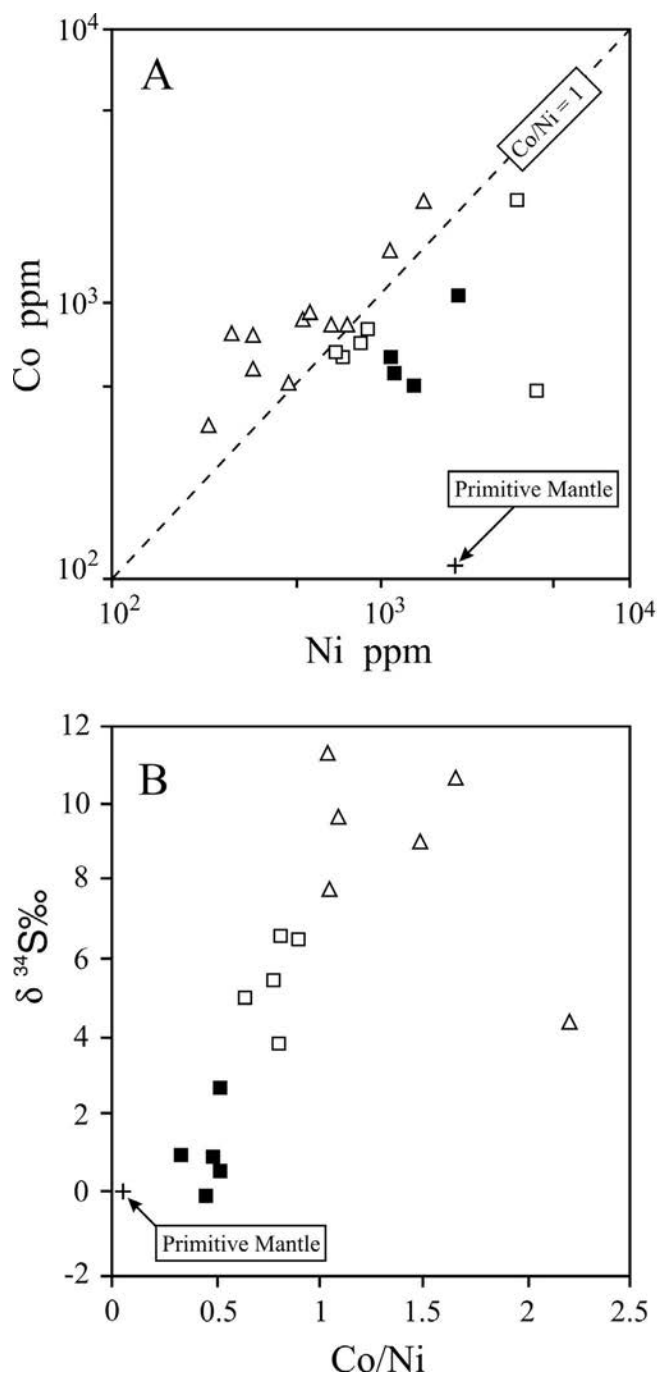
Fig. 13 - Co-Ni (A) and Co/Ni-δ^{34}S (B) relationships in pyrite from hydrothermal stockwork veins of the Northern Apennine ophiolites. Open triangles- basalt-hosted veins; open squares- serpentinite-hosted veins; black squares- magmatic sulfides in serpentinite; cross- primitive mantle, from Barrie and Hannington (1999).

tramafic rocks are significantly altered at relatively high temperatures (250-350°C) and water/rock ratios (Shanks et al., 1981; Reed, 1983). The H$^+$ required for sulfate reduction is supplied by reduction of H$_2$O mainly through oxidation of Fe^{2+} in mafic minerals (olivine, orthopyroxene, spinels) or volcanic glass, and removal of Mg^{2+} from seawater to form secondary hydrous silicates (serpentine, talc, chlorite). During reaction, the hydrothermal solution becomes more and more acid due to increasing activity of H$^+$. Fe^{2+} is dissolved as hydroxide complexes, whereas base metals (i.e., Cu, Zn)

are stored in the solution mainly as hydrochloride complexes (Reed, 1983). The solution becomes also enriched in silica, and loses Mg, Ca, Na and SO$_4^{2-}$ that is reduced to S^{2-} through the simplified reaction:

$$2H^+ + SO_4^{2-} + 4H_2 \rightarrow H_2S + 4H_2O$$
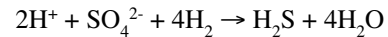
Isotopic fractionation normally reaches maximum $\Delta_{H2S-SO4}$ factors of approximately -20‰ (Ohmoto and Goldhaber, 1997). Isotopic ratios of Northern Apennine stockwork ores vary in the range +3.9‰ and +11.4‰, indicating $\Delta_{H2S-SO4}$ values between -13.14‰ and -5.64‰ with respect to coeval seawater sulfate (Fig. 11). These values are consistent with the proposed mechanism of inorganic sulfate reduction, but do not exclude mixing with sulfur derived from leaching of the country rock sulfide with δ^{34}S lighter than the seawater sulfate.

The average δ^{34}S of sulfides from serpentinite-hosted veins (+5.9‰) is one third less than the average δ^{34}S of basalt-hosted stockwork deposits (+8.9%), ranging from +3.9‰ to +6.7‰. Excluding mixing processes with biogenic or magmatic sulfur, this variation may represent a decrease of δ^{34}S downwards in the stratigraphic succession. This feature, already observed elsewhere, is interpreted as a result of mixing with increasing amounts of descending fresh seawater, when the ascending hydrothermal solution approaches the seafloor (Green et al., 1981; Huston et al., 1995). In the serpentinite-hosted veins of the Northern Apennine it may also indicate an Early Jurassic age of the serpentinite-hosted deposits that would imply initially lighter δ^{34}S (~15.88‰) for the 200 Ma seawater (Fig. 11). However, given the close time-relation between deposition of the stockwork veins and Upper Jurassic basaltic magmatism, the low δ^{34}S of sulfides from serpentinite-hosted veins has to be ascribed to some different process. We suggest that it was due to relatively high mixing rates with sulfur derived from leaching of sulfide minerals within the ultramafic country rocks, having almost chondritic δ^{34}S ratios, similar to the sulfides from the "il Pozzo" deposit. Zaccarini and Garuti (2008) have shown that chemical and mechanical interaction with rocks of predominant ultramafic composition variably enriched the serpentinite-hosted veins in compatible metals (i.e., Ni, Cr, Mg). Among other effects, these deposits display a lower Co/Ni ratio of pyrite compared with deposits hosted in basalt (Table 3, Fig. 13A). Consistently, the δ^{34}S of pyrite correlates with the Co/Ni ratio increasing from pyrite in magmatic deposits to pyrite in basalt-hosted veins (Fig. 13B). The intermediate composition of pyrite from serpentinite-hosted veins suggests a possible mixing process between two end members represented by hydrothermal and magmatic sulfur, respectively.

Seafloor stratiform deposits: the role of organic matter

The δ^{34}S data graphically summarized in Fig. 12 show that the trend defined by stockwork and stratabound hydrothermal deposits is abruptly interrupted by the stratiform deposits associated with the serpentinite and basalt breccias, both showing distinctive shifting of δ^{34}S from +7.5‰ downwards, into the negative field (to δ^{34}S = -2.9‰). Structural and sedimentary features recognized within and around the stratiform deposits indicate that their stratigraphic position corresponds to ancient seafloor.

In general, discharge of sulfides at ocean-floor vents occurs as a result of mixing between hydrothermal solutions and cold seawater that causes a sharp drop in T and an increase in pH. Under these conditions, base metals (i.e., Cu

and Zn), which are mainly transported as hydrochloride complexes, are readily precipitated as insoluble sulfides (Reed, 1983; Lyndon, 1988; Rona, 1988; Scott, 1997; Seward and Barnes, 1997). The final δ^{34}S of the precipitating sulfides depends on the rate of mixing between the two end-members, eventually implying an enrichment in the heavy ^{34}S isotope derived from in-situ reduction of fresh seawater sulfate. A major implication is that seafloor sulfides may have δ^{34}S ratios even higher than those precipitating in a sub-seafloor environment. For example, this could be the case of sample BD6 from Monte Bardeneto (Table 4) in which the pyrite has a δ^{34}S of +7.5‰, slightly higher than the maximum value recorded in veins emplaced in the ultramafic substrate (+6.7‰). However, most isotopic values obtained from stratiform sulfides of the Apennine show a variable enrichment in the light ^{32}S isotope, up to reach negative δ^{34}S ratios. Excluding mixing with juvenile sulfur, both the depositional environment and the abundance of biogenic features (Figs. 4 to 8) suggest that lightening of sulfur isotope ratios might have resulted from mixing of hydrothermal and biogenic sulfur, the latter typically having $\Delta_{\text{H2S-SO4}}$ as negative as -45‰ (Ohmoto and Goldhaber, 1997).

Stratiform sulfides were deposited on the seafloor together with clastic material eroded from the footwall breccia and remnants of planktonic biota (Garuti and Zaccarini, 2005; Zaccarini and Garuti, 2008). In submarine conditions, the organic debris started to decompose yielding H$^+$ for in situ reduction of the seawater sulfate:

(1) $\qquad (CH_2O) + H_2O \rightarrow 4H^+ + CO_2$

(2) $\quad 2(CH_2O) + SO_4^{2-} \rightarrow 2H^+ + S^{2-} + 2H_2O + 2CO_2$
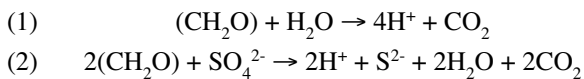
Initially, sulfate reduction might have occurred in the absence of bacteria (reaction 1), being controlled by thermal decomposition of organic matter at relatively high temperatures (T° > 230°C, pH < 2). This reduction pathway, however, would have not caused substantial isotopic fractionation, since the resulting sulfides would have approached the isotopic composition of the SO_4^{2-} reservoir (Ohmoto and Goldhaber, 1997). The observed enrichment in light ^{32}S is better explained by reaction (2) driven by anaerobic "sulfate-reducing-bacteria" (SRB), at temperatures below 110°C (upper life-limit for thermophilic SRB). The SRB generate the energy essential to their life by oxidizing organic matter via reduction of the seawater sulfate molecule SO_4^{2-}. The relevant metabolic waste product of this biochemical process is S^{2-} which, in the surrounding of seafloor vents is fixed within the crystal framework of precipitating sulfide minerals together with the inorganic-reduced S^{2-} present in hydrothermal fluids. Since the chemical linkages ^{32}S-O in the sulfate molecule are weaker than the ^{34}S-O bonds, they are more easily broken by SRB. Accordingly, the resulting S^{2-} is isotopically lighter than the initial aqueous sulfate by highly negative sulfide/sulfate fractionation factors ($\Delta_{\text{H2S-SO4}}$ = -45‰). The reaction also yields CO_2 that contributes to precipitation of abundant calcite observed in the matrix of the stratiform deposits of the Northern Apennine.

According to this model, SRB were directly responsible for oxidation of the organic matter coating the internal wall of microfossil shells, thereby precipitating metal sulfides that resulted in the pseudomorphic replacement of the original structure (pyritization of microfossils at Corchia and Reppia II). Furthermore, bacteria cells played a passive role in the mineralizing reactions by acting as templates for deposition of metals. For example, bacteria can modify the chemical properties in the immediate environment (i.e., pH, Eh, S^{2-} activity) as a
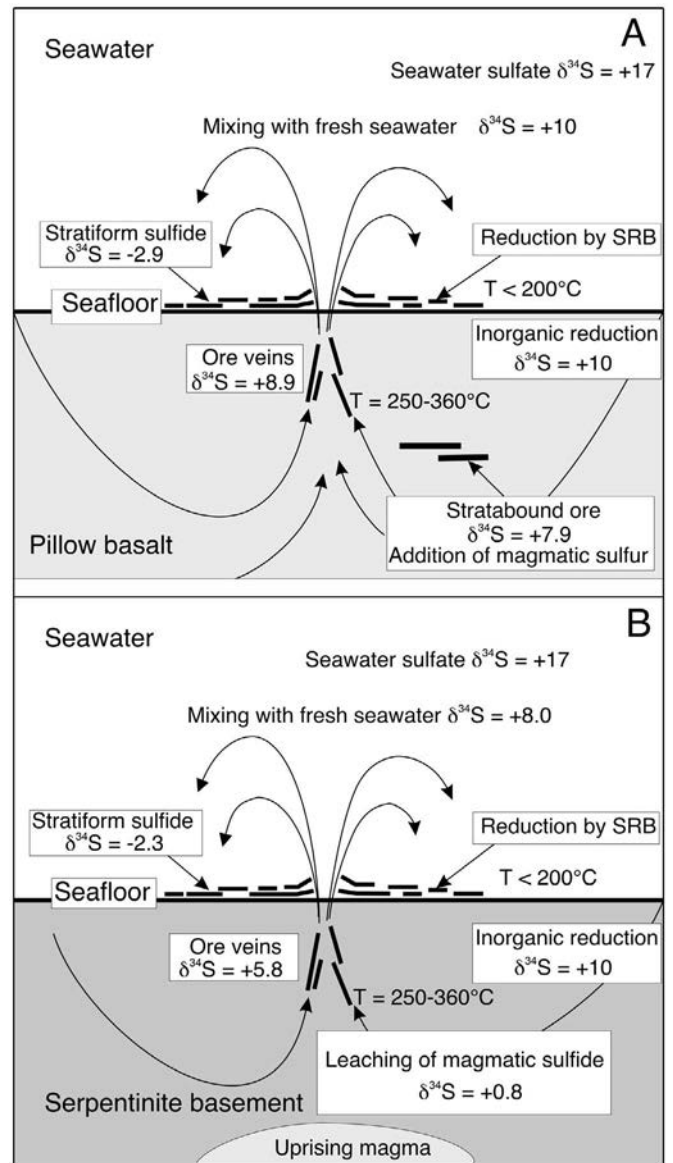

Fig. 14 - Schematic model illustrating the origin of δ^{34}S variations in the Northern Apennine VMS deposits. The initial value of δ^{34}S ~ 17 assumed for seawater sulfate at 165 Ma has been extrapolated from the evolution curve of Claypool et al. (1980) in Fig.10. T = temperature of sulfide deposition inferred from chlorite geothermometry (see text). A) Distribution of δ^{34}S in basalt-hosted sulfide deposits: stratabound ore and ore veins have similar δ^{34}S, derived from inorganic reduction of seawater sulfate during convection through the basalt substrate. B) Distribution of δ^{34}S in serpentinite hosted sulfide deposits: the low δ^{34}S in ore veins is caused by leaching of magmatic sulfides during convection through the serpentinite substrate. In both cases A and B, seafloor stratiform deposits have very low δ^{34}S, down to negative values, derived from syngenetic, biogenic reduction of seawater sulfate.

result of their metabolic activity, thereby creating very restricted sites for local precipitation of metals (Konhauser, 1998). The numerous microstructures observed in the Ligurian stratiform deposits (spherules, coronas, filaments) might have originated in this way. Their morphology and size strongly recall bacteria cells completely encrusted with microgranular crystallites (in our case pyrite, sphalerite, magnetite) observed in nature and in experimental cultures (Konhauser, 1998 and references therein). In our samples, textural features indicate that biogenic ore minerals are usually associated with either pure silica or silicates dominated by the Fe-

Al assemblage (possibly chlorites or clay-like phases) that form thin films coating the sphalerite spheroids and the infilling of spherules and capsular aggregates. The infilling silicate is always associated with dusty disseminated Fe-sulfide particles, and overall differs in chemistry and mineralogy from the external matrix enclosing the corona aggregates, which consists of dominant calcite with subordinate amounts of quartz and chlorite. The general context suggests that the silicate infilling of spherules and corona aggregates may represent material nucleated by microorganisms. This conclusion is supported by experimental studies (Urrutia and Beveridge, 1994) showing that some bacteria are able to flock (Fe-Al) silicates around their bodies with retention of considerable amounts of heavy metals, including Zn, Cd, Ni, Cu and Pb. Filament and spheroid microstructures consisting of iron and silica or Si-Al-Fe compounds, similar to those described here, have been reported from ancient and modern hydrothermal vents, including deep-sea hot springs of the northwest Pacific Ocean and lava flows of the Juan de Fuca Ridge (Konhauser, 1998; Juniper and Fouquet, 1988). In all cases, the microstructures were recognized as the result of biocatalyzed precipitation of inorganic compounds (sulfides, oxides, silicates).

The magnetite-silicate spherules in sample BD8 from Monte Bardeneto closely recall in shape and size the Fe-oxide spheroids from the Precambrian banded iron formations (Laberge et al., 1987), and analogously they are interpreted as bacteria-induced mineralization. Magnetite microspherules (10-50 μm) have been observed as a by product of organic matter oxidation by anaerobic bacteria in experimental cultures (Konhauser, 1998), according to the following possible reaction:

$$CH_3COO^- + 8Fe(OH)_3 \rightarrow 8\ Fe^{2+} + 2HCO_3^- + 15\ OH^- + 5H_2O$$
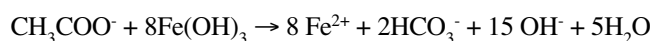
This reaction is favoured by relatively high pH, a condition commonly met at the seafloor, and requires a solid source of Fe^{3+} (i.e., ferrihydrite) to sustain the production of oxygen for oxidation of organic matter, and of Fe^{2+} for precipitation of magnetite.

At Monte Bardeneto, the ore texture suggests that magnetite and hematite associated with primary sulfides (pyrrhotite, chalcopyrite, pyrite) formed initially through inorganic processes involving a change in redox conditions from anoxic-suboxic to oxic. This change was probably not due to a variation in the composition of the hydrothermal fluid itself, more likely it was reflecting progressive recession from the venting site toward a more marginal zone, in which oxic conditions were prevailing. The early formed iron oxides (hematite and magnetite) provided the solid source of Fe^{3+} to be reduced for oxidation of the organic matter and crystallization of the magnetite byproduct. Magnetite precipitated by the biologically-induced process assumes the typical spheroid shape with Fe-Al silicate infillings similar to the sulfide-silicate spherules produced by SRB. Sample BD8 contains both types of spherules (sulfide and oxide) concentrated in adjacent domains. We suggest that the magnetite spherules may have formed as a continuum of the sulfide biomineralization process that characterizes the zones more proximal to the venting site. Magnetite-producing bacteria are able to live above and below the anoxic-oxic boundary (Konhauser, 1998). Interestingly, it has been observed in nature that one single bacterium can produce Fe-sulfide or Fe-oxide under anoxic or oxic conditions, respectively, thus implying that a local variation in O^{2-} to HS^- activity was the factor controlling the type of excreted iron species (Bazylinski et al., 1990).

SUMMARY AND CONCLUSIONS

Sulfur isotope values in VMS deposits of the Northern Apennine ophiolites have an overall average of 5.9 δ^{34}S‰, similar to other VMS deposits of the eastern Mediterranean Tethys, i.e. Troodos (4.6‰) and Eastern Turkey (4.2‰). They differ, however, for a much wider range of δ^{34}S, varying from +11.4‰ to -2.9‰. The origin of this variation is schematically represented in Fig. 13, assuming an initial δ^{34}S value of 17‰ for seawater at 165 Ma.

The highest δ^{34}S‰ values (average 8.9‰) are found in sulfide ores occurring as stockwork veins or stratabound bodies within the pillow basalt unit (Fig.13A). These values are consistent with partial inorganic reduction of seawater sulfates during convective circulation through the basaltic substrate, plus a possible addition of magmatic sulfur in the stratabound ores. A significant decrease of the average δ^{34}S ratio to 5.8‰ and 2.5‰ is observed in sulfides from serpentinite-hosted stockwork veins and stratiform deposits lying on ancient seafloor, respectively. In the first case, sulfur derived from the leaching of magmatic sulfides, characterized by an almost chondritic δ^{34}S ratio of 0.8‰, was added to the hydrothermal fluids while they migrated through the serpentinite basement (Fig.13B). In the second case, ^{32}S was most likely contributed to the sulfide ore by the action of SRB. Because of the weak post-depositional recrystallization of the ore, many of the primary structures were exceptionally preserved and interpreted as produced by bacterial activity. They indicate that the light isotope was derived from syngenetic, biogenic reduction of seawater sulfate, and mixed with hydrothermal inorganic sulfur at the time of sulfide precipitation on the seafloor. Probably, biologic-driven isotopic reworking of the stratiform sulfides continued during the long-lasting exposure at the seafloor, before burial under basalt lava flows and pelagic sediments.

The results of this isotopic investigation provide further evidence for the influence of the country rock type (basalt vs. serpentinite) and the depositional setting (seafloor vs. subseafloor) on the ore composition in the Northern Apennine VMS deposits.

ACKNOWLEDGEMENTS

REFERENCES

Abbate E., Bortolotti V., Passerini P. and Sagri M., 1970. Introduction to the geology of the Northern Apennine. In: G. Sestini (Ed.), Development of the Northern Apennine geosyncline. Sedim. Geol., 4: 207-249.

Barrett T.J., 1982. Review of stratigraphic aspects of the ophiolitic rocks and pelagic sediments of the Vara complex, North Apennines, Italy. Ofioliti, 7 (1): 3-46.

Barrett T.J. and Friedrichsen H., 1989. Stable isotopic composition of atypical ophiolitic rocks from east Liguria, Italy. Chem. Geol., 80: 71-84.

Barrie C.T. and Hannington M.D., 1999. Classification of volcanic-associated massive sulfide deposits based on host-rock composition. In: C.T. Barrie and M.D. Hannington (Eds.), Volcanic-associated massive sulfide deposits: processes and examples in modern and ancient settings. Rev. Econ. Geol., 8: 1-11

Bazylinski D.A., Frankel R.B., Garrat-Reed A.J. and Mann S., 1990. Biomineralization of iron sulfides in magnetotactic bacteria from sulfidic environments. In: R.B. Frankel and R.P. Blakemore (Eds.), Iron biominerals. Plenum Press, New York, p. 239-255.

Bertolani M., 1952. I giacimenti cupriferi nelle ofioliti di Sestri Levante. Per. Mineral., 21 (2/3): 149-170.

Bertolani M., 1953. I giacimenti cupriferi dell'Appennino Modenese. Ricerche microscopiche a luce riflessa. Atti Soc. Nat. Mat. Modena, 82: 3-10.

Bertolani M., 1959. Ricerche sulle rocce prasinitiche e anfibolitiche e sul giacimento metallifero di Vigonzano (Appennino piacentino). Atti Soc. Nat. Mat. Modena, 89/90: 3-31.

Bertolani M., 1962. Linneite, calcopirrotina e strutture blenda-pirrotina nelle mineralizzazioni metallifere del giacimento di Corchia (Appennino Parmense). Per. Mineral., 31 (2/3): 287-301.

Bertolani M. and Capedri S., 1966. Le ofioliti delle province di Modena e Reggio Emilia. Atti Soc. Nat. Mat. Modena, 97: 3-52.

Bonatti E., Zerbi M., Kay R. and Rydell H., 1976. Metalliferous deposits from the Apennine ophiolites: Mesozoic equivalents of modern deposits from oceanic spreading centers. Bull. Geol. Soc. Am., 87: 83-94.

Bortolotti V. and Gianelli G., 1976. Le rocce gabbriche dell'Appennino settentrionale: I dati recenti su rapporti primari, posizione stratigrafica ed evoluzione tettonica. Ofioliti, 1: 99-105.

Bortolotti V., Cellai D., Vaggelli G., Villa I.M., 1991. ^{40}Ar/^{39}Ar dating of Apenninic ophiolites: 2. Basalts from the Aiola sequence, Southern Tuscany. Ofioliti, 16: 37-42.

Cabella R., Lucchetti G. and Marescotti P., 1998. Mn-ores from Eastern Ligurian ophiolitic sequences ("Diaspri di Monte Alpe" formation, Northern Apennines, Italy). Trends in Mineral., 2: 1-17.

Capedri S. and Toscani, L., 2000. Subduction-related (?) ophiolitic metabasalts from Northern Apennines (Modena Province, Italy). Chem. Erde, 60: 111-128.

Claypool G.E., Hosler W.T., Kaplan I.R., Sakai H. and Zak I., 1980. The age curves of sulfur and oxygen isotopes in marine sulfate and their mutual interpretation: Chem. Geol., 28: 199-260.

Cortesogno L., Gianelli G. and Piccardo G.B., 1975. Petrogenesis and metamorphic evolution of the ophiolitic mafic rocks (Northern Apennine and Tuscany). Boll. Soc. Geol. It., 94: 291-327.

Dal Piaz G.V., 1974a. Le métamorphisme alpin de haute pression et basse temperature dans l'évolution structurale du bassin ophiolitique alpino-apenninique. 1e partie: Boll. Soc. Geol. It., 93: 437-468.

Dal Piaz G.V., 1974b. Le métamorphisme alpin de haute pression et basse temperature dans l'évolution structurale du bassin ophiolitique alpino-apenninique. 2e partie. Schweitz. Mineral. Petrol. Mitt., 57: 59-88.

Ferrario A., 1977. Metallogeny of the Italian ophiolites. In: S. Jancovic (Ed.), Metallogeny and plate tectonics in the northeastern Mediterranean. IGCP Correlation Project Nr.3, Faculty Mining Geol., Belgrade, p. 369-382.

Ferrario A. and Garuti G., 1980. Copper deposits in the basal breccias and volcano-sedimentary sequences of the Eastern Ligurian ophiolites (Italy). Mineral. Deposita, 15: 291-303.

Francheteau J. and 14 others, 1979. Massive deep-sea sulphide ore deposits discovered on the East Pacific Rise. Nature, 277: 523-528.

Galli M. and Penco A.M., 1996. Le miniere di rame e di manganese della Liguria orientale. Atti Acc. Ligure Sci. Lett., serie V, 53: 215-247.

Galley A.G. and Koski R.A., 1999. Setting and characteristic of ophiolite-hosted volcanogenic massive sulfide deposits. In: C.T. Barrie and M.D. Hannington (Eds.), Volcanic-associated massive sulfide deposits: processes and examples in modern and ancient settings. Rev. Econ. Geol., 8: 221-246.

Garuti G. and Zaccarini F., 2005. Minerals of Au, Ag, and U in volcanic-rock-associated massive sulfide deposits of the Northern Apennine ophiolite, Italy. Can. Mineral., 43: 935-950.

Garuti G., Alfonso P., Zaccarini F. and Proenza J.A., 2007. Sulphur-isotope variations in seafloor and subseafloor, Cyprus-type VMS deposits of the Northern Apennine ophiolites (Italy): preliminary results. In: C.J. Andrew et al. (Eds.), Digging deeper. Proc. Ninth Biennal SGA Meeting, Dublin 2007, 2: 1041-1044.

Garuti G., Bartoli O., Scacchetti M. and Zaccarini F., 2008a. Geological setting and structural styles of volcanic massive sulfide deposits in the Northern Apennines (Italy): evidence for seafloor and sub-seafloor hydrothermal activity in unconventional ophiolites of the Mesozoic Tethys. Bol. Soc. Geol. Mex., 60 (1): 121-145.

Garuti G., Adorni F., Calderini V. and Zaccarini F., 2008b. L'oro del "Pozzo": secondo ritrovamento di oro nativo nell`ofiolite di Corchia, Berceto (Appennino Parmense). Micro, 2: 133-144.

Giesemann A., Jäger H.J., Norman A.L., Krouse H.R. and Brand W.A., 1994. On-line sulfur-isotope determination using an elemental analyzer coupled to a mass spectrometer. Anal Chem., 66: 2816-2819.

Goodfellow W.D. and Zierenberg R.A., 1999. Genesis of massive sulfide deposits at sediment-covered spreading centers. In: C.T. Barrie and M.D. Hannington (Eds.), Volcanic-associated massive sulfide deposits: processes and examples in modern and ancient settings. Rev. Econ. Geol., 8: 297-324.

Green G.R., Solomon M. and Walshe J.L., 1981. The formation of the volcanic-hosted massive sulfide at Rosebery, Tasmania. Econ. Geol., 76: 304-338.

Huston D.L., 1999. Stable isotopes and their significance for understanding the genesis of volcanic-hosted massive sulfide deposits: a review. In: C.T. Barrie and M.D. Hannington (Eds.), Volcanic-associated massive sulfide deposits: processes and examples in modern and ancient settings. Rev. Econ. Geol., 8: 157-179.

Huston D.L., Sie S.H., Cooke D.H., Both R.A. and Suter G.F., 1995. Trace elements in sulfide minerals from eastern Australian volcanic-hosted massive sulfide deposits: Part II. Selenium levels in pyrite: Comparison with δ^{34}S values and implications for the source of sulfur in volcanogenic hydrothermal systems. Econ. Geol., 90: 1185-1196.

Juniper S.K. and Fouquet Y., 1988. Filamentous iron-silica deposits from modern and ancient hydrothermal sites. Can. Mineral., 26: 859-869.

Kranidiotis P. and McLean W.H., 1987. Systematic of chlorite alteration at the Phelps Dodge massive sulfide deposit, Matamagi, Quebec. Econ. Geol., 82: 1898-1911.

Konhauser K.O., 1998. Diversity of bacterial iron mineralization. Earth Sci. Rev., 43: 91-121.

Laberge G.L., Robbins E.I. and Han T.M., 1987. A model for the biological precipitation of Precambrian iron-formations. A geological evidence. In: P.W. Uitterdijk and G.L. Laberge (Eds.), Precambrian iron-formations. Theophrastus Publ. Athens, p. 69-96.

Lagabrielle Y. and Lemoine M., 1997. Alpine, Corsican and Apennine ophiolites: the slow-spreading ridge model. C.R. Acad. Sci., Paris, 325: 909-920.

Lemoine M., Tricart P. and Boillot G., 1987. Ultramafic and gabbroic ocean floor of the Ligurian Tethys (Alps, Corsica, Apennines): In search of a genetic model. Geology 15: 622-625.

Leoni L., Sartori F. and Tamponi M., 1998. Compositional variation in K-micas and chlorites coexisting in Al-saturated metapelites under late diagenetic to low-grade metamorphic conditions (Internal Liguride Units, Northern Apennines, Italy). Eur. J. Mineral., 10: 1321-1339.

Lyndon J.W., 1988. Volcanogenic massive sulphide deposits. Part 2. Genetic models. Geosci. Can., 15: 43-65

Maggi R. and Pearce M., 2005. Mid fourth-millennium copper mining in Liguria, north-west Italy: the earliest known copper mines in Western Europe. Antiquity, 79: 66-77

Marcucci M. and Passerini P., 1991. Radiolarian bearing siliceous sediments in the Mesozoic of the Northern and Central Apennines. Ofioliti, 16: 121-126.

Moretti, E., 1937. Autarchia Mineraria. L'Industria Miner. It. Oltremare, 11 (1): 12-16.

Ohmoto H., 1986. Stable isotope geochemistry of ore deposits. In: J.W. Valley, J.H.P. Taylor ad J.R. O'Neil (Eds.), Stable isotopes in high temperature geological processes. Mineral. Soc. Am. Rev.,16: 491-560.

Ohmoto H. and Goldhaber M.B., 1997. Sulphur and carbon isotopes. In: H.L. Barnes (Ed.), Geochemistry of hydrothermal ore deposits. 3rd Ed., John Wiley & Sons, p. 517-611.

Piccardo G.B., Rampone E. and Romairone A., 2002. Formation and composition of the oceanic lithosphere of the Ligurian Tethys: inferences from the Ligurian ophiolites. Ofioliti, 27 (2): 145-161.

Pipino G., 2003. Oro, miniere, storia - Miscellanea di giacimentologia e storia mineraria italiana. Monogr. Mus. Storico Oro Italiano, Lerma (Alessandria), 510 pp.

Reed M.H., 1983. Seawater-basalt reaction and origin of greenstones and related ore deposits. Econ. Geol., 78: 466-485

Rona P.A., 1988. Hydrothermal mineralization at oceanic ridges. Can. Mineral., 26: 431-466.

Rye O.R., 2005. A review of the stable-isotope geochemistry of sulfate minerals in selected igneous environments and related hydrothermal systems. Chem. Geol., 215: 5-36.

Sandrone R., Leardi G., Rossetti P. and Compagnoni R., 1986. P-T conditions for the eclogite re-equilibration of the metaophiolites from Val d'Ala di Lanzo (Internal Piedmontese Zone, Western Alps). J. Metam. Geol., 4: 161-178.

Sangster D.F., 1968. Relative sulphur isotope abundances of ancient seas and strata-bound sulphide deposits. Proc. Geol. Ass. Can., 19: 79-91.

Scott S.D., 1997. Submarine hydrothermal systems and deposits. In: H.L. Barnes (Ed.), Geochemistry of hydrothermal ore deposits. 3rd Ed., John Wiley & Sons, p. 797-875.

Seward T.M. and Barnes H.L., 1997. Metal transport by hydrothermal ore fluids. In: H.L. Barnes (Ed.), Geochemistry of hydrothermal ore deposits. 3rd Ed. John Wiley & Sons, p. 435-486.

Seyfried W.E. Jr., Kang Ding, Berndt M.E. and Xian Chen, 1999. Experimental and theoretical controls on the composition of mid-ocean ridge hydrothermal fluids. In: C.T. Barrie and M.D. Hannington (Eds.), Volcanic-associated massive sulfide deposits: processes and examples in modern and ancient settings. Rev. Econ. Geol., 8: 181-200.

Shanks III W.C., Bishoff J.L. and Rosenbauer R.J., 1981. Seawater sulfate reduction and sulfur isotope fractionation in basaltic systems: interaction of seawater with fayalite and magnetite at 200-350°C. Geochim. Cosmochim. Acta, 45: 1977-1995.

Solomon M., 1976. 'Volcanic' massive sulfide deposits and their host rocks. A review and explanation. In: K.H. Wolf (Ed.), Handbook of stratabound and stratiform ore deposits. Elsevier, 6: 21-50.

Tribuzio R., Tiepolo M. and Vannucci R., 2000. Evolution of gabbroic rocks from the Northern Apennine ophiolites (Italy): Comparison with the lower oceanic crust from modern slow-spreading ridges. In: J. Dick, E. Moores, D. Elthon, A. Nicolas (Eds.), Ophiolites and oceanic crust: New insights from field studies and Ocean Drilling Program. Geol. Soc. Am. Spec. Pap., 349: 129-138.

Tribuzio R., Thirlwall M.F. and Vannucci R., 2004. Origin of the gabbro-perdotite association from the Northern Apennine ophiolites (Italy). J. Petrol., 45 (6): 1109-1124.

Urrutia M.M. and Beveridge T.J., 1994. Formation of fine grained metal and silicate precipitates on a bacterial surface (*Bacillus subtilis*). Chem. Geol., 116: 261-280.

Violi Guidetti L., 1968. Le miniere di Val Dragone. Atti Mem. Deput. Storia Patria, 10: 369-378.

Zaccarini F., 2006. Accessory minerals in volcanic massive sulfide deposits of the Northern-Apennine ophiolites (Italy): their petrogenetic significance. Resum. Comunic., 26 Reunion (SEM) / 20 Reunion (SEA). Macla, 6: 505-508.

Zaccarini F. and Garuti G., 2008. Mineralogy and composition of VMS deposits of Northern Apennine ophiolites, Italy: evidence for the influence of country rock type on ore composition. Miner. Petrol., 94: 61-83.

Zaccarini F., Garuti G., Rossi A., Carrillo-Rosua F.J., Morales-Ruano S. and Fenoll Hach-Ali P., 2003. Application of chlorite and Fluid-inclusion geothermometry to vein and stratiform Fe-Cu-Zn sulfide deposits of theNorthern Apennine Ophiolites (Emilia-Romagna and Liguria, Italy). Atti Ticinensi Sci. Terra, 9: 109-111.